THESIS

UNCOUPLING PLANT GROWTH AND DEFENSE THROUGH PHYTOHORMONE CROSSTALK MODIFICATION

Submitted by

Grace A. Johnston

Department of Agricultural Biology

In partial fulfillment of the requirements

For the Degree of Master of Science

Colorado State University

Fort Collins, Colorado

Spring 2023

Master's Committee:

Advisor: Cris Argueso

Jan Leach
Ashok Prasad

ABSTRACT

UNCOUPLING PLANT GROWTH AND DEFENSE THROUGH
PHYTOHORMONE CROSSTALK MODIFICATION

Phytohormones are essential regulators of development and response to biotic and abiotic stresses. Activation of the plant immune system by pathogen attack often results in changes in plant growth, frequently leading to smaller plants with reduced seed set. Previously, we discovered that cytokinin (CK), a hormone known for its role in the regulation of cell division and plant growth, also has an important role in the activation of defense against pathogens through a synergistic interaction with the defense hormone salicylic acid (SA). Here, we address whether these two phytohormones also regulate the negative effect of immune activation on plant growth. Differential gene expression analysis and physiological assays were used to characterize the crosstalk between CK and SA in growth and defense in *Arabidopsis thaliana* plants with altered states of immunity. We show that the interplay between the phytohormones CK and SA regulates both defense responses to pathogens and plant development. Endogenous levels of these two hormones were modulated in the *snc1 ckx3 ckx5* (*s35*) triple mutant. The three mutations result in increased CK and SA content simultaneously and yields a novel reproductive growth phenotype. When challenged with pathogens from diverse lifestyles, the *s35* mutant conserves an autoimmune phenotype. Transcriptome analysis of *s35* reproductive tissue reveals differential regulation of genes associated with nitrogen response and regulation of redox status. Our data suggests that the increased content of both CK and SA hormones contributes to a rebalancing of redox homeostasis and perception of nutrient availability within the shoot apical meristem (SAM), resulting in the uncoupling of reproductive growth and pathogen defense. Further experimentation and investigation into the

mechanistic interactions mediating the balance between plant growth and defense could lead to implementation of phytohormone crosstalk engineering to target specific advancements in crop species.

ACKNOWLEDGEMENTS

I would like to express my deepest gratitude to my graduate advisor, Dr. Cris Argueso. Without your relentless encouragement, I would have never undertaken my journey through graduate school or even into the realm of plant biology. Additionally, I would like to extend my sincere thanks to my other committee members: Dr. Jan Leach and Dr. Ashok Prasad. I appreciate your feedback and commitment to this work.

Special thanks to the members of the Argueso Lab, past and present. It truly takes a village to “raise” a competent scientist, and each of you have majorly contributed to my scientific foundation. Thanks, team!

I was honored to be funded by the National Science Foundation via the Graduate Research Fellowship in 2020. I am very appreciative of the support NSF granted me and my research.

Lastly, I would be remiss in not mentioning the unwavering support and love from my friends and family. Behind the scenes, y’all have kept me fed, laughing, and motivated throughout. I am eternally grateful.

TABLE OF CONTENTS

1. BACKGROUND

The plant growth-defense tradeoff

As plants have evolved over millions of years, they have gained unique survival strategies to cope with changes in environment and interactions with other organisms. Due to their sessile lifestyle, plants have evolved to utilize complex signaling pathways to respond to abiotic and biotic stresses. The selective pressures plants experience are unique to prevailing environmental conditions, resource availability, and physiological confines, and thus require plasticity to adapt to these constraints. To ensure resilience, plants rely on tradeoffs as coordinated tactics to mitigate harm caused by sub-optimal conditions and overcome resource limitations.

Scientists have long been aware of the interplay between evolution, ecology, and plant genetics for optimized growth and survival. There are several known plant tradeoffs, yet the most prominent is the growth-defense tradeoff, in which there is a cost to growth and development associated with activation of defense responses to pathogens and pests (Coley et al., 1985; Bergelson & Purrington, 1996). This evolutionary plant survival strategy is complex and requires tight regulation of cellular signaling systems. Within this area of research, there are historically two main hypotheses regarding the evolutionary relevance for the growth-defense tradeoff: favoring of offensive plant processes or favoring of defensive plant processes, or, as Monson et al., 2021 describes using economic allegory, supply-side processes and demand-side processes. Tradeoff hypotheses that involve offensive plant processes emphasize resource partitioning as it pertains to the plant's selective pressures. As explained in Huot et al., 2014, the energy harvested from photosynthesis contributes to a finite pool of resources that are diverted to either growth or defense depending on the presence or absence of a pathogen, a process mediated by phytohormone signaling. Conversely, hypotheses favoring defensive plant processes are centered around selective pressures on the plant pathogen and/or herbivore.

Instead of resource allocation, plants optimize defense chemical allocation to specific tissues on the basis of importance for reproduction and likelihood of infection or wounding (Rhoades, 1979; Zangerl & Bazzaz, 1992).

Yet, the canonical model of mutual antagonism between growth and defense has been challenged, as in Kliebenstein, 2016. The author postulates whether it is a misconception to view the relationship between growth and defense as perpetually opposing forces and provides examples that do not display this tradeoff, suggesting that these two plant processes are instead in continual dialogue to ensure plasticity in a fluctuating environment (Kliebenstein, 2016). Furthermore, Monson et al., 2021 provides evidence for the unification of the offensive and defensive tradeoff hypotheses, using a multi-omics approach. In this study, the authors use the evolutionary optimization framework employed by both types of hypotheses to combine transcriptomics, pathway networking, and genetic mutation analyses. They put forth a new hypothesis, the coordinated resource allocation hypothesis, in which the growth-defense tradeoff has multiple levels of regulation, i.e. hormone crosstalk, transcriptional cascades, that contribute to an effective response to stress, all while maintaining a safety resource reserve to ensure phenotypic plasticity (Monson et al., 2021).

Regardless, the relationship between development and immunity can be partially attributed to phytohormone signaling pathways. Different hormone families regulate specific physiological processes individually. Nonetheless, it has been shown that phytohormones act in synergistic networks for refined decision-making (de Vleesschauwer, Gheysen, & Höfte, 2013; Yang et al., 2013; Altmann et al., 2020). In particular, the crosstalk between cytokinin (CK) and salicylic acid (SA) is also associated with the growth-defense tradeoff. Historically, CK has been known for its positive regulation of plant growth, while SA initiates plant defense responses during pathogen attack. Previously, it was discovered that these hormones may intervene with each other's signaling pathways, suggesting they have pleiotropic qualities. CK assists in plant-pathogen interactions by potentiating defense signaling, whereas SA suppresses CK

responsiveness (Argueso et al., 2012). These findings propelled us to further elucidate the CK-SA crosstalk and its dynamic capacity in fine-tuning plant growth and defense for environmental adaptation. Implicating the relationship as a nexus for growth-defense homeostasis, we propose, in this work, that the CK-SA crosstalk can be modulated for a desired phenotypic outcome.

Cytokinin

The discovery of CKs in the late 1950s and early 1960s was of great interest to plant scientists, as these compounds were shown to stimulate plant cell proliferation, first identified in *Nicotiana tobacum* (Miller et al., 1956). Though there are multiple forms of plant-derived CKs, all variations structurally consist of an adenine with a modified N^6 terminus (Kudo et al., 2010). There are two groups of CKs characterized by the N^6 terminus substitutions: isoprenoid and aromatic. While CKs with aromatic derivative side chains are only found in a few plant species, isoprenoid CKs are abundant. During isoprenoid CK biosynthesis, adenosine phosphate-isopentenyltransferase (IPT) catalyzes the conjugation of the CK nucleotide to the isoprenoid precursor, dimethylallyl pyrophosphate (DMAPP), consuming either adenosine triphosphate (ATP) or adenosine diphosphate (ADP) in the process. This reaction yields N^6-(Δ^2-isopentenyl)adenine (iP) nucleotides. The isoprenoid side chain of iP can be *trans*-hydroxylated to produce *trans*-Zeatin (tZ) nucleotides by a cytochrome P450 enzyme. iP and tZ are the two most abundant forms of CK in plants relative to the other isoprenoid CKs, *cis*-Zeatin (cZ) and dihydrozeatin (DZ) (Hirose et al., 2008).

In plants, CKs can be metabolically converted between nucleotide, nucleoside, and glucoside conjugates (reviewed in Sakakibara, 2006). Biologically active CKs are formed by the conversion of nucleotides to nucleobases. Two pathways of CK activation have been recorded, a two-step pathway and a direct pathway. The two-step pathway includes, first, a dephosphorylation step and then, deribosylation. Conversely, CK riboside 5'-monophosphate

phosphoribohydrolase (LONELY GUY; LOG) catalyzes the production of CK nucleobases in a single reaction. Storage forms of CKs are formed by *O*-glycosylation and cannot trigger downstream CK signaling. Although reactivation of *O*-glycosylated forms by β-glucosidases can occur, *N*-glycosylation of the purine is permanent. To further regulate hormone homeostasis, CK degradation is mediated by CK oxidase/dehydrogenase (CKX) enzymes. CKXs cleave the isoprenoid side chains of active CKs and their nucleosides, although they cannot act on DZ and aromatic CKs and have a lower affinity to cZ as compared to iP and tZ.

Similar to the regulatory mechanism of prokaryotes, CK signal transduction is through a two-component phosphorelay (reviewed in Kieber & Schaller, 2014). Active forms of CK bind to sensor domains on transmembrane histidine kinases (HKs), which then activates autophosphorylation of a histidine residue on the intracellular transmitter domain and subsequently an aspartate on the receiver domain. The phosphoryl group is then transferred to a histidine phosphotransferase (HP), which carries the signal from the cytosol into the nucleus. Response regulators (RRs) are phosphorylated by HPs, inducing transcription of cytokinin-regulated genes and downstream signaling. In *Arabidopsis thaliana* (Arabidopsis), there are two subfamilies of RRs: type-A and type-B Arabidopsis RRs (ARRs). While type-B ARRs are transcription factors and positive regulators of CK responses, type-A ARRs cannot bind DNA and act in a negative feedback loop to regulate CK signaling. Type-B ARR binding sites are found in the promoter regions of type-A *ARR* genes, and type-B ARR proteins can directly regulate type-A *ARR* transcription, suggesting a mechanism of fine-tuning of CK responses.
CK has been associated with many plant processes, primarily growth and development. CK treatment has inverse growth regulation in shoots versus roots: CK promotes shoot growth but inhibits root growth (Werner et al., 2003). Loss-of-function mutants of type-B *ARR*s are vegetatively stunted (Ishida et al., 2008), whereas constitutive ectopic expression of a type-B using the cauliflower mosaic virus (CaMV) *35S* promoter leads to larger shoot mass compared to wildtype (Zubo et al., 2017). Similarly, disruption of the degradation enzymes, CKXs, causing

overaccumulation of CK, results in increased reproductive activity, as in the rice *OsCKX2* mutant (Ashikari et al.,2005; Tsago et al., 2020) and the Arabidopsis *ckx3 ckx5* double mutant (Bartrina et al, 2011). Both mutants have increased seed number, as CK mediates meristematic activity of developing reproductive tissue.

Furthermore, CK functions in nutrient allocation throughout the plant (reviewed in Sakakibara, 2021) and during immune responses (reviewed in McIntyre, Bush, & Argueso, 2021). As nitrogen availability signals, tZ and tZ riboside are translocated from root-to-shoot via the xylem to modulate plant growth and development (Sakakibara, 2006). It is also well-documented that some plant pathogens manipulate host machinery to increase local CK levels. This, in turn, activates cell division and creates a nutrient sink to benefit the pathogen. While treatment of low concentrations of CK can make plants more susceptible to pathogens (Babosha, 2009; Argueso et al., 2012; Chanclud et al., 2016), application of high CK concentrations can lead to the potentiation of defense responses, such as production of reactive oxygen species (ROS) and activation of defense gene expression through interaction with other defense hormones (Choi et al., 2010; Argueso et al., 2012).

Salicylic Acid

SA and its related forms have been medicinally utilized by humans indirectly for centuries. As a naturally occurring phytohormone, SA was concentrated in teas and tinctures for treatment of various ailments by soaking, oil extraction, and maceration of plant tissue like willow (*Salix* genus). After SA was isolated and identified, bulk synthesis and mass production of its derivatives became prevalent as an active ingredient for pharmaceutical use, such as widely utilized aspirin tablets. As SA has played a crucial role in the history of medicine, it, likewise, is essential to plant survival. Within the plant, SA functions in pathogen response and disease resistance.

Plant-derived SA is proposed to be biosynthesized in two separate pathways, though, both start with chorismate, an intermediate in the Shikimate pathway of aromatic amino acid metabolism (Peng et al., 2021). Though, the prevalence of the two pathways of SA biosynthesis varies amongst plant species (reviewed in Hartmann & Zeier, 2019; Lefevere, Bauters, & Gheysen, 2020). In the isochorismate synthase pathway, chorismate is converted to isochorismate by the isochorismate synthase (ICS) enzyme, and then into SA by isochorismate pyruvate lyase. Alternatively, the conversion of chorismate to phenylalanine can then be used a substrate of phenylalanine ammonia lyase (PAL). SA is produced after further β-oxidation and hydroxylation reactions. Although a recent study has contradicted the role of PAL in SA biosynthesis in Arabidopsis (Wu, Zhu, & Zhao, 2022), it is thought to be the primary synthesis pathway in rice species. Thus, the complexities of these pathways are not ubiquitous amongst all land plants and require further investigation.

During normal growth and development, basal SA levels are at low concentrations in the plant. Once a pathogen is perceived, SA biosynthesis and metabolism are rapidly upregulated, in conjunction with other defense metabolites, like ROS. As SA accumulates, the proposed SA receptor, NONEXPRESSER OF PR GENES 1 (NPR1), is monomerized, activated after binding, and translocated to the nucleus. NPR1, along with other transcriptional activators, particularly TGACG- binding transcription factors (TGAs), recruit RNA polymerase II to initiate SA-dependent gene expression, like *PATHOGENESIS-RELATED* (*PR*) genes.

Initiation of plant immune responses by recognition of pathogens and pathogen-associated molecular patterns is a complex process that requires a high level of signaling control throughout the plant (Dodds & Rathjen, 2011). The timely and dynamic nature of SA signaling is key to defending against biotrophic or hemibiotrophic pathogen attack, locally and systemically. SA majorly contributes to defense signal transduction to distal, unchallenged tissues during systemic acquired resistance (SAR). Overactivation of immunity can come at a cost to the plant. Mutants with overaccumulation SA or overactivation of SA signaling have

dwarfed phenotypes (Zhang et al., 2003). Likewise, application of benzothiadiazole (BTH), a synthetic analog of SA, can reduce plant biomass (Canet et al., 2010). The mechanisms associated with growth inhibition by SA is believed to be in relation to crosstalk with other hormones.

Targeting phytohormone crosstalk as a tool for agricultural advancement

Agricultural practices have evolved over centuries and allowed for the human population to grow exponentially. The vast majority of land use by humans is for agricultural purposes, including farming, animal grazing, and logging territories (Easterling et al., 2007). Yet, with climate change and the steady increase of the human population, the demand for viable crop yield is at an all-time high. Although agricultural methods, like selective breeding, soil fertilization, and pesticide application, have improved production of major crops over the past several decades, they are not sustainable to meet the requirements for the projected human population and are unlikely to withstand the changing climate (Ray et al., 2012, 2013; Ning, Liu, & Wang, 2017). Breeding programs have historically selected for growth-related crop improvements, at the expense of genetic variation that lends to immune resilience (Strange & Scott, 2005). Additionally, plants can be more susceptible to pathogen attack in heat conditions (reviewed in Cohen & Leach, 2020), an intensified risk to crop populations with the unprecedented increase of global temperatures (Allen et al., 2018). Thus, further progress in this field is urgent and necessary to assure global food security.

The cost of immune activation has been well-documented, in crop species and model plants alike, and often results in changes in plant growth and development, frequently leading to smaller plants with reduced seed set (Brown, 2002; van Wersch, Li, & Zhang, 2016). Conversely, plants overexpressing transporters of secondary metabolites resulting in overactive growth are more susceptible to biotic attack (Tiwari et al., 2014). Mitigation of the growth-defense tradeoff has been particularly difficult due to the pleiotropic nature of genes activated in

both processes. For example, ROS are critical signaling molecules that are dual-natured in that they can be activated during both development and defense pathways (Apel & Hirt, 2004).

The mechanisms driving phytohormone crosstalk can happen at many levels, and resulting phenotypes are products of the complex action by several phytohormone pathways. One strategy to manipulate hormone crosstalk is to target expression of transcription factors, reviewed in Berry & Argueso, 2022. These proteins directly bind to DNA, initiating transcriptional cascades in response to stimuli. Several studies have proved this to be a successful method of regulating hormone crosstalk, as some transcription factors play dual roles in positively regulating both growth and immunity (Winter et al., 2011, Yan et al., 2020, Xiao et al., 2021). Another idea is to alter interactions between signaling proteins. Altmann et al., 2020 showed that phytohormones have extensive protein networks and suggested modification to protein-protein interactions between two or more phytohormone pathways could provide novel phenotypic outcomes. Here, we provide evidence of phytohormone crosstalk engineering to overcome the growth-defense tradeoff. In our approach, we target endogenous phytohormone concentration in order to modify signaling interactions between two phytohormones, CK and SA.

2. INTRODUCTION

Phytohormones are small molecules that regulate a plethora of plant physiological processes, from development to responses to the environment. Moreover, phytohormones can trigger signaling cascades and, therefore, act in interacting networks for refined plant cell decision-making (Altmann et al., 2020). This is the case during organogenesis; above ground plant organs (leaves, stem, flowers, etc.) originate from meristematic tissue called the shoot apical meristem (SAM). SAM activity is determinate of proper vegetative growth, as well as reproductive yield (fruit production and seed set), which are agronomically important traits. A complex genetic network of phytohormones has been shown to regulate the stem cell domain, namely, CK and auxin (Su, Liu, & Zhang, 2011). CK controls stem cell proliferation and, therefore, meristem size. It has been shown that disruption of CK signaling or accumulation, such as with mutations in the CK biosynthesis genes *IPT*s, results in growth retardation (Miyawaki et al., 2006). Conversely, overaccumulation of endogenous CKs (Bartrina et al., 2011) or overexpression of CK-triggered transcription factors that activate mitosis (Yang et al., 2021b) yield larger meristems and increased cell numbers.

Phytohormones play a significant role in pathogen sensing and downstream responses. When a microbe is present, the plant immune system is strategically activated in waves. PAMP-triggered immunity (PTI) is initiated when plant cells recognize specific pathogen-associated molecular patterns (PAMPs). With PTI activation, plants respond with upregulation of induced defenses, such as production of ROS. In response, pathogenic microbes have developed ways to overcome PTI by the secretion of effectors, molecules that can target and manipulate plant physiology to benefit the pathogen, known as effector-triggered susceptibility (ETS). Subsequently, this initiates effector-triggered immunity (ETI) in the host plant, as host resistance (*R*) genes perceive effector presence. Many of these *R* genes encode nucleotide-binding

leucine-rich repeat proteins (NLRs) that trigger ETI-mediated responses like *PR* gene expression, hypersensitive response (HR), and accumulation of the defense hormone SA.

Notably, it has been shown that both PTI and ETI activation often result in changes in plant growth and development, frequently leading to smaller plants with reduced seed set (Gómez-Gómez et al., 1999; Tian et al., 2003; van Wersch, Li, & Zhang, 2016). Likewise, Arabidopsis mutants with constitutive activation of defense responses and over-accumulation of SA have similar developmental retardation (Bowling et al., 1994, 1997; Li et al., 2001). This has been associated with the growth-defense tradeoff survival strategy. Amongst the known interactions between hormones, the crosstalk between CK and SA is of particular interest in relation to this tradeoff. Although, CK is known for its role in the regulation of cell division at the meristem level and overall plant growth, it has also been shown to play an important role in the activation of defense, through cooperative interaction with the defense hormone SA (Argueso et al., 2012). In contrast, it has been proposed that high SA content and/or signaling has inhibitory effects on the CK pathway, resulting in fitness costs (Argueso et al., 2012). This suggests that these two phytohormones may be at the crux of the mechanistic components plants use to maintain a balance between adequate defense activation and growth and reproduction.

Phytohormones and their associated genetic hubs have been proposed as potential targets for plant bioengineering (Berry & Argueso, 2022). Using reserve genetics, our aim is to provide preliminary evidence of a reestablished phytohormone homeostasis for a preferred outcome, suggesting that phytohormone engineering for crop improvement is possible. Here, we show that the manipulation of both the CK and SA pathways leads to perturbation of the growth-defense tradeoff, conferring mutant plants with high pathogen resistance and high reproductive yield. In addition, the unique hormone balance of our genetic combination results in distinct physiological and metabolic deviations of nitrogen perception and redox status. By furthering investigations of the complex network of interactions mediating the balance between

plant growth and defense, future efforts in synthetic biology can be used to develop advanced crops with increased pathogen resistance, superior plant yield, and abiotic stress resistance.

3. METHODS

Plant materials & growth conditions

All plant lines are in the Columbia-0 ecotype. *snc1-1* (Li et al., 2001) and *ckx3-1 ckx5-1* (Bartrina et al., 2011) acquired from Dr. Thomas Schmülling from Freie Universität Berlin. Plants were crossed, resulting in the *snc1 ckx3 ckx5* (*s35*) mutant, which was genotyped by PCR for homozygosity (see genotyping primers in Table 1). Plants were grown in growth chambers in long day conditions (16 h light/8 h dark, 22°C) unless otherwise stated. Light intensity was 120-150 μE. Relative humidity was held at 55% day/65% night. For pathogen assays, plants were grown in short day conditions (8 h light/16 h dark, 22°C) with all other growth conditions kept consistent. Plants were watered with tap water, unless alternatively specified. For fertilization experiments, plants were given 1X Miracle-Gro Water Soluble All Purpose Plant Food (24-8-16) when pots were dry.

Hormone treatment

Hormone solutions were made using Sigma-Aldrich 6-benzylaminopurine (BA) and salicylic acid (SA). Dimethyl sulfoxide (DMSO) was used as the solvent. Dilutions were made in DI water. Spray treatments were done using Prevail sprayers. For liquid hormone treatment, seedlings were grown vertically on MS plates for two weeks and transferred to liquid MS media for a 1 h acclimation period under growth chamber lighting (long day conditions described above), shaking at 75 rpm. Hormone was then added to flasks to the final concentration indicated. Seedlings were incubated to the specified times under growth chamber lighting shaking at 75 rpm.

Scanning electron microscopy

Primary shoot apical meristems of 6-week-old plants were hand dissected to stage 6 buds (Smyth et al., 1990). Meristems were then fixed in 100% dry methanol for 10 minutes, then 100% dry ethanol for 30 minutes two times. Samples were critically dried with ethanol as the transitional fluid. Meristems were mounted upright on SEM stubs and gold coated. Images were captured using JEOL JSM-6500 Field Emission Scanning Electron Microscope at Colorado State University.

RNA isolation & qRT-PCR

All plant tissue types were ground frozen using a tissue lyser and total RNA was extracted using the Qiagen RNeasy Mini Kit. RNA quality was assessed by A_{260}/A_{280} and A_{260}/A_{230} ratios via a NanoDrop. RNA samples of acceptable quality were treated with Invitrogen TURBO DNase as per manufacturer's instructions. DNase treated RNA was checked for genomic DNA contamination by qRT-PCR using primers for *ACTIN* (AT5G66770). cDNA was synthesized using Quantabio QScript per manufacturer's instructions. cDNA was checked for full extension using three *PP2A* (AT1G13320) amplicons 1 kB apart. cDNA samples with C_q differences between primer pairs below 1.5 were acceptable for qRT-PCR gene expression. All qRT-PCR was performed using Quantabio PerfeCTa SYBR Green FastMix on Bio-Rad CFX Connect Real-Time PCR System, with CFX Maestro Software used for analysis. *UBIQUITIN 10* (AT4G05320) was used as a reference gene in all experiments. All qRT-PCR primer sequences are provided in Table 2.

RNA sequencing

All samples were collected developmentally, when the primary shoot had at least one fully expanded flower (Stage 13+) was present (Smyth et al., 1990). Inflorescences were dissected to Stage 12 and under and cut from the stem. Between 15-18 inflorescences were

pooled per sample. Samples were ground frozen using a tissue lyser and total RNA was extracted using the Qiagen RNeasy Micro Kit. RNA quality was assessed by A_{260}/A_{280} and A_{260}/A_{230} ratios via a NanoDrop and RIN_e scores via an Agilent 4150 TapeStation. RNA was sent to Novogene for RNA sequencing. Raw reads were filtered using fastp (Chen et al., 2018) by removing reads containing adapters, reads containing N > 10%, and low-quality reads. Paired-end clean reads were mapped to the TAIR10 reference genome (Berardini et al., 2015) using HISAT2 software (Kim et al., 2019). RPKM of each gene was calculated using featureCounts (Liao et al., 2014). Benjamini and Hochberg's approach for controlling the False Discovery Rate (FDR) by the DESeq2 R package (Love, Huber, & Anders, 2014) was used to determine genes with an adjusted P value < 0.05 and were assigned as differentially expressed. Gene ontology (GO) enrichment analysis of differentially expressed genes was performed using PANTHER 17.0 database (http://go.pantherdb.org/; Thomas et al., 2022). GO terms with an FDR corrected P value < 0.05 were considered significantly enriched.

Hyaloperonospora arabidopsidis inoculation & trypan blue staining

Hyaloperonospora arabidopsidis Noco2 (*Hpa*) was propagated on the susceptible Col-0 accession. Two-week-old plants were sprayed with *Hpa* spores ($5x10^4$/mL) using a pressurized sprayer (Preval). Inoculated plants were covered with a transparent plastic dome to maintain high humidity. One day after the first appearance of sporangiophores (6 dpi) the first pair of true leaves was collected from three individual plants and added to a previously weighed 1.7 mL microcentrifuge tube containing 300 µL of sterile water, for a total of six leaves per sample, and weighed again to determine fresh weight. Spores were counted using a hemacytometer. Spore counts from at least four samples per genotype were determined.

For trypan blue staining, plants were harvested at 4 dpi and stained with a 3:1 ethanol:lacto-phenol trypan blue solution (1:1:1:1 phenol:lactic acid:water:glycerol and 0.05% trypan blue (Sigma-Aldrich)), at 95°C, for 5 minutes, and moved to room temperature for 10

minutes. Excess staining was removed with 15 M chloral hydrate (Sigma-Aldrich). Samples were moved to 50% glycerol for storage and mounting. Pictures were taken with a Nikon DS-Fi2 Microscope CCD camera mounted on a Nikon SMZ18 stereomicroscope.

Hydrogen peroxide staining

Using a modified protocol from Daubi & O'Brien, 2012, primary inflorescences from 6-week-old plants were stained with 1 mg/mL 3,3-diaminobenzidine (DAB) solution overnight on a laboratory shaker. The next day, samples were cleared with 3:1:1 enthanol:acetic acid:glycerol bleaching solution overnight on a laboratory shaker. The bleaching solution was replaced as needed. After clearing all chlorophyll, samples were preserved in 50% glycerol. Pictures were taken with a Dino-Lite Edge^{Plus} 1.3MP AM4917 Series microscope.

***TCSn::GFP* imaging**

Wildtype and transgenic *TCSn::GFP* seedlings (Zürcher et al., 2013) were grown vertically on MS plates supplemented with either water (mock) or 50 μM SA for 10-14 days. Seedling roots were mounted on slides and imaged using a Leica DM 5000-D fluorescence optical microscope.

***Pseudomonas syringae* inoculation**

Plants were germinated on pots covered with a plastic mesh. Two-week-old seedlings were watered in the morning of the inoculation day. Plants were dip-inoculated with a bacterial suspension as described by (Tornero & Dangl, 2001) with noted changes. *Pseudomonas syringae* pv. *tomato* DC3000 EV (*Pst*) was streaked from 50% glycerol stock solution kept at -80^{o} C on King's B (KB) Media supplemented with Rifampicin (50 mg/mL) and Kanamycin (50 mg/mL) and incubated for 24 hours at 28^{o} C. 24 hours before inoculation a lawn plate of *Pst* was streaked onto a new $KB_{rif,kan}$ plate and incubated at 28^{o} C. On the day of inoculation, the bacteria

were resuspended in 10 mM $MgCl_2$ for a bacterial concentration of $1x10^6$ CFU/mL (equivalent to OD_{600} = 0.0002). Plants were inoculated by dipping the top of the pot into the bacterial solution for 5 seconds. After bacterial dip, plants were covered with a lightly sprayed dome for 24 hours post inoculation (hpi), which was then cracked for 24 h, and removed 48 hpi. The amount of in planta bacteria was quantified 1 hpi (day 0) and 3 days post inoculation (dpi). Multiple seedlings were pooled for one sample, three or four samples were collected for each genotype/treatment at each time point. Tissue was ground in 10 mM $MgCl_2$ and serial dilutions were used to determine the CFU/mg fresh weight (FW). Day 0 dilutions were plated on KB plates containing kanamycin and rifampicin, and day 3 dilutions were plated on KB plates containing rifampicin and cycloheximide, incubated at 28°C for 24-48 hours before colony counting for CFU determination.

Botrytis cinerea **inoculation**

Botrytis cinerea B10.5 (*B. cinerea*) sclerotia obtained from Dr. Dan Kliebenstein at the University of California, Davis. *B. cinerea* was grown on 0.5X Potato Dextrose Agar (PDA) plates until sporulation. A spore solution of $0.5x10^4$ spores/mL was prepared in ½ strength organic grape juice (R.W. Knudson Family Organic Juice, Just Concord) and 0.05% tween. The spore solution was sprayed on 6-week-old plants using a Prevail sprayer. Plants were placed in a flat under a water-sprayed plastic dome to maintain humidity. Pictures of plants were taken at 96 hpi. Plants were analyzed by the percentage of necrotic tissue of the rosette, and each plant was qualitatively assigned to one of the five disease index categories (20%, 40%, 60%, 80%, and 100% of leaves displaying disease symptoms). Disease indexes were averaged per genotype and a two-way ANOVA analysis with biological replicate as a blocking factor was performed to evaluate significance.

Hormone quantification

For SA and JA quantification, leaf tissue from 6-week-old plants, or primary inflorescences from 8-week-old plants were dissected to Stage 15 buds (Smyth et al., 1990), were collected. All samples were immediately flash frozen in liquid nitrogen after harvest and later lyophilized. Three independent biological samples were harvested from each genotype. Leaves from three plants (or approximately 30 inflorescences) were pooled per replicate. Tissue samples were homogenized and extracted with organic solvents, and LC-MS/MS analysis was performed on a Waters Acquity Classic UPLC coupled to a Waters Xevo TQ-S triple quadrupole mass spectrometer at the Colorado State University Bioanalysis and Omics (ARC-BIO) facility (Sheflin et al., 2019).

For CK quantification, primary inflorescences were collected as described above. Sample extraction and cytokinin quantification using the methods described in Kojima et al., 2009. A Waters Xevo TQ-S quantitative mass spectrometer and Waters Acquity UPLC HSS T3 (1.8 μm, 2.1 x 100 mm) column were used.

4. RESULTS

Salicylic acid inhibits cytokinin signaling

Previous work demonstrated that the phytohormones CK and SA positively crosstalk in defense responses of Arabidopsis against pathogens, with CK acting to potentiate SA responses in the presence of pathogen attack (Argueso et al., 2012). Moreover, mutants with decreased SA content (*eds16*, harboring a loss-of-function mutation in the SA biosynthetic gene *ISOCHORISMATE SYNTASE 1*) showed increased sensitivity to CK, indicating that SA has an inhibitory effect on CK signaling (Argueso et al., 2012). Given the importance of CK to plant growth, we hypothesized that a negative interaction of SA on CK signaling could be partially responsible for the growth tradeoffs usually associated with immune activation.

To understand the interaction between SA and CK on plant growth, we analyzed publicly available gene expression data (Bio-Analytic Resource; http://bar.utoronto.ca; Toufighi et al., 2005) for changes in the expression of cytokinin-regulated genes (including CK signaling, biosynthesis, and degradation genes) after SA treatment. Three hours after application of 10 μM SA, most of the genes investigated were markedly downregulated (Figure 1A), suggesting that exogenous application of SA to Arabidopsis plants has an inhibitory effect on the expression of genes in the CK signaling and metabolic pathways. To address whether genetic manipulations leading to SA overaccumulation also inhibit CK signaling, the autoimmune mutants *constitutive expressor of PR genes 1* (*cpr1*), *cpr5*, and *suppressor of npr1-1 constitutive 1* (*snc1*), known to have elevated levels of SA and constitutive defense activation (Clarke et al., 2000; Li et al. 2001), were examined for their levels of CK-regulated transcripts. Leaf tissue of three-week-old wildtype, *cpr1*, *cpr5*, or *snc1* mutants was harvested to examine basal expression of the CK-regulated genes *ARABIDOPSIS RESPONSE REGULATOR 7* (*ARR7*), *CYTOKININ OXIDASE 4* (*CKX4*), *CYTOKININ RESPONSE FACTOR 6* (*CRF6*), and *EXPANSIN 1* (*EXP1)*. Results in Figure 1B show that, for the most part, these mutants displayed a general inhibition of CK-

regulated gene expression, consistent with the phenotypes associated with these pleiotropic mutations, in which general activation of defense responses is observed. To further evaluate CK-regulated gene responsiveness to SA, we performed timecourse liquid hormone induction assays. Arabidopsis seedlings were grown on Murashige and Skoog medium (MS) vertical plates for two weeks and transferred to liquid MS media. One hour after transfer to liquid media, 100 μM SA or a 0.01% DMSO vehicle control were added to the media. Tissue was then harvested at different times after hormone or 0.01% DMSO control addition, over the course of 24 hr. Both *ARR7* and *CRF6* were downregulated in the presence of SA at each timepoint, beginning 15 minutes after SA treatment (Figure 1C). Similarly, *EXP1* was downregulated by SA treatment at most of the timepoints. These data recapitulate results obtained from publicly available data (Figure 1A) and demonstrate that the suppression of CK-regulated gene expression by SA occurs rapidly upon hormone perception.

We then investigated whether this rapid suppression of CK signaling by SA treatment could be maintained over time, or whether it was relieved shortly after stimulus perception. To address this question we used *TCSn::GFP* transgenic plants, harboring a synthetic transcriptional reporter for CK signaling, which allows for visualization of CK responses *in planta*. Transgenic *TCSn::GFP* Arabidopsis plants, or Col-0 untransformed controls, were grown for 10-14 days on vertical MS plates supplemented with either water (mock) or 50 μM SA. CK signal was detected using fluorescent microscopy. Mock treated *TCSn::GFP* plants showed intense accumulation of *GFP* localized at the root tip (Figure 1D), as expected due to localized CK signaling (Aloni et al., 2005). When compared to the mock treated plants, roots treated with SA showed reduced *GFP* intensity. Taken together, these experiments show that SA can quickly repress CK gene transcription, and that this suppression is maintained over extended periods of time, as long as the SA stimulus is present.

Phytohormone crosstalk engineering

With the above-described hormone interactions in mind, we hypothesized that the disruption of the native negative crosstalk of SA on CK signaling could influence plant growth during active states of immunity, relieving the growth-defense tradeoff. Given that the molecular mechanisms of this negative crosstalk are currently unknown, we addressed the relief of this negative regulation by engineering the crosstalk through changes in hormone quantity, rather than signaling. Cytokinin oxidases/dehydrogenases (CKX) mediate the cleavage of the isoprenoid side chains of active CKs and their nucleosides, rendering the resulting CK species biologically inactive (Galuszka et al., 2007). In Arabidopsis, CKXs are encoded by a gene family of 7 members, and loss-of-function mutations in *CKX* genes result in increased CK content, due to decreased degradation of CKs (Werner et al., 2003; Galuszka et al., 2007; Bartrina et al., 2011). We therefore hypothesized that reducing CKX activity in backgrounds with high levels of SA could render plants with increased cytokinin content, surpassing the suppression of growth by SA during immunity activation. In order to engineer the crosstalk, we first addressed the tissue-specificity and developmental regulation of *CKX* gene expression in Arabidopsis, by analysis of publicly available gene expression data (Bio-Analytic Resource; http://bar.utoronto.ca/; Toufighi et al., 2005). Analysis of the expression patterns of *CKX* genes revealed that *CKX3* and *CKX5* are predominantly expressed in reproductive tissues (Figure 2). Thus, *CKX3* and *CKX5* are good candidates for CK-dependent regulation of reproductive growth.

suppressor of npr1-1 constitutive 1 (*snc1-1*) is an autoimmune mutant, which harbors a gain-of-function mutation in an NLR protein, leading to constitutive defense activation, high SA content, and dwarfed morphology (Li et al., 2001). Conversely, a double mutant harboring T-DNA mutations in *CYTOKININ OXIDASE 3* and *5* (*ckx3,5*) exhibits increased content of biologically active forms of CK, increased number of inflorescence meristems, increased number of flowers, and increased seed yield (Bartrina et al., 2011). We crossed *snc1* and

ckx3,5 plants, and the resulting F2 plants were genotyped to identify *snc1-1, ckx3-1, ckx5-1* homozygous triple mutants, using Cleaved Amplified Polymorphic Sequence (CAPS) markers (Table 1). The resulting triple mutant, which we named *s35*, was then characterized.

_s35_ displays a novel reproductive growth phenotype

Similar to the *snc1* mutant, *s35* exhibits a dwarfed vegetative morphology, with approximately 55% reduction of rosette growth compared to wildtype (Col-0) (Figure 3A and 3B). Although *s35* rosettes can be larger than *snc1*, it is not significant (Figure 3B). Given that *CYTOKININ OXIDASE 3* and *5* are mostly expressed in reproductive tissue (Figure 2), reproductive growth parameters of *s35* plants were also assessed for any growth penalties (Figure 3C to 3H). *s35* retains the reduced apical dominance phenotype characteristic of *snc1* plants (Li et al., 2001), with reduced primary stem growth (Figure 3E) and more than double the number of secondary lateral shoots compared to wildtype (Figure 3F). At the terminal end of shoots, *s35* plants display novel silique growth patterns. The seed pods are compressed as the internodes between successive organs are drastically reduced. This results in a distinctive radial-like silique growth pattern at the shoot apex we coined the “starburst” phenotype (Figure 3D). The starburst phenotype has an altered penetrance in primary shoots versus secondary shoots, with about 55% of primary shoots and about 71% of secondary shoots displaying the starburst phenotype (Figure 4A).

As fitness is arguably the most important agronomic trait, we assessed reproductive yield characterization of the genotypes. Siliques from 12-week-old plants were counted, measured, and harvested for seed. *ckx3,5* had significantly increased silique number on the primary stem and overall compared to wildtype (Figure 3G). We found that the *snc1* mutant had a significant reduction in silique number, characteristic of the autoimmune reproductive phenotypes previously observed in this background (Li et al., 2001). In contrast, the silique

count of *s35* was similar from that of Col-0, suggesting that an increase in CK content could rescue the reduction seed production observed in the *snc1* background.

In addition to silique production, *s35* had over double (almost 260%) the seed yield compared to *snc1* (Figure 3H). When individual siliques were assessed, *s35* and *snc1* had about 50% shorter siliques compared to wildtype (Figure 4B). Moreover, *s35* had an increase in aborted ovules in dissected siliques, with almost half the number of viable seed per valve in comparison to Col-0 (Figure 4C and 4D). Taken together, these factors likely contribute to the loss of seed production in the *s35* mutant as compared to Col-0 (Figure 3H).

In addition, we also crossed *ckx3,5* to *cpr1* in order to determine if the starburst phenotype was SNC1-dependent. *cpr1 ckx3,5* (*c35*) had inflorescences that resemble those of *s35* (Figure 5). Thus, this altered reproductive phenotype is likely due to the combinatorial effects of the *ckx3,5* mutations and autoimmunity.

_s35_ has a reestablished hormone homeostasis in the SAM

To determine if the starburst phenotype of the *s35* mutant was the result of alteration in the SAM, scanning electron microscopy (SEM) of SAMs was conducted (Figure 6A to 6E). *ckx3,5* displayed increased meristem diameter and floral organ primordia compared to Col-0, as previously described (Figure 6F) (Bartrina et al., 2011). The *snc1* mutant had a reduced meristem size compared to Col-0, implicating SA as a negative regulator of meristematic growth. Most notably, *s35* meristems often had remarkably altered meristematic growth: some meristems displayed the wildtype phenotype (Figure 6D), while others had severely compacted floral organ primordia of many stages (Smyth et al., 1990), swollen sepals, and deviation from the typical SAM phyllotactic pattern (Figure 6E). As the plant matures, this irregular meristematic patterning likely contributes to the distinctive *s35* starburst silique phenotype (Figure 3D).

Because CK is known to play a large role in meristematic maintenance (Perales & Reddy, 2012), CK species were quantified in inflorescence tissue by mass spectrometry to identify possible changes in CK homeostasis in the *s35* background (see Table 3 for absolute quantities of all species measured). The main bioactive forms of CK are considered to be *trans*-Zeatin (tZ) and N^6-(Δ^2-isopentenyl)adenine (iP), with potentially differing roles (Kudo et al., 2010). tZ-type precursor CKs (most often tZ-riboside) are thought to travel from the root to the shoot in xylem tissue, during nutrient sensing (Miyawaki et al., 2004; Takei et al., 2004), while iP-type CKs move from shoot to root in the phloem. Quantification of CK species in the *ckx3,5* reproductive tissues showed that *ckx3,5* plants had higher levels of tZ and tZ-type CKs, both precursor and inactivated species, comparatively to wildtype (Figure 6G). Similarly, *s35* also displayed increased levels of tZ-type CKs. iP-type CKs were at relatively low levels compared to tZ-types in all genotypes, although *s35* had significantly higher levels of inactivated iP-type species compared to all genotypes, suggesting possible modifications to CK translocation signaling in the triple mutant.

The understanding of how defense hormones, like SA and jasmonic acid (JA), influence SAM development is lacking. Thus, we also quantified these hormones in inflorescence tissue. *snc1* reproductive tissue had the highest accumulation of SA, whereas *ckx3,5* had the lowest (Figure 6H). If SA acts to repress meristem activity, either directly or indirectly, this disparity could underline the dwarfed versus enlarged SAM phenotypes characteristic of *snc1* and *ckx3,5*, respectively (Figure 6B and 6C). Moreover, Col-0 and *s35* had intermediate SA content, similar to their intermediate SAM phenotypes (Figure 6A and 6D). JA was higher in the *ckx3,5* and *s35* inflorescences, suggesting CK may have the ability to promote JA accumulation. As shown, the *s35* mutant has a unique hormone profile in the inflorescence that likely contributes to its novel reproductive growth phenotype.

***s35* has broad spectrum resistance to pathogens**

It is well documented that *snc1* plants have increased resistance to biotroph pathogens, such as *Pseudomonas syringae* pv. *tomato* DC3000 (*Pst*) and *Hyaloperonospora arabidopsidis* Noco2 (*Hpa*) (Li et al., 2001). We wanted to identify whether the increased endogenous levels of CK due to the *ckx3,5* mutations, altered the *snc1* defense phenotype. Two-week-old plants were inoculated with *Hpa* and spore count was recorded six days post inoculation (dpi). On average, *s35* had roughly half the number of spores when compared to wildtype, indicating significantly increased resistance on par with *snc1* plants (Figure 7A). Further, *Hpa* inoculated plants were stained with trypan blue for pathogen structure visualization. Wildtype and *ckx3,5* showed widespread hyphal and sporangiophore production, whereas *snc1* and *s35* did not. To test resistance against a hemibiotrophic pathogen, two-week-old plants were dip inoculated with *Pst*. Similarly to the *Hpa* assays, *snc1* and *s35* displayed decreased susceptibility to this pathogen, with statistically less bacterial growth at 3 dpi as compared to *ckx3,5* and the wildtype (Figure 7B). A characteristic of the *snc1* mutant is the constitutive activation of defense genes, such as *PATHOGENESIS-RELATED 1* (*PR1*) (Li et al., 2001). We found that untreated *s35* plants have similar constitutive activation of *PR1* to that of the *snc1* mutant (Figure 8). When treated with *Pst*, *snc1* and *s35* showed even higher levels of *PR1* expression when compared to mock treatment (Figure 7C). To further characterize the defense phenotypes, basal SA in untreated leaf tissue was quantified. *snc1* had statistically higher levels of SA compared to the other genotypes, as expected (Figure 7D). Notably, *s35* also had elevated levels of SA, reflecting its autoimmune phenotype.

Increased resistance to biotrophic pathogens is usually accompanied by increased susceptibility to necrotrophs, due to the antagonistic interaction between the SA and JA pathways. The increased resistance to biotrophs observed in the *s35* mutant prompted us to determine its susceptibility to necrotrophs. Rosettes of wildtype, *ckx3,5*, *snc1*, and *s35* plants were inoculated with the necrotizing fungus *Botrytis cinerea* by spray inoculation. *snc1* had

roughly 40% more lesion-covered rosette area than wildtype plants (Figure 9A). Although *s35* was more susceptible to *B. cinerea* than wildtype by 27%, it was less susceptible than *snc1* by about 10%. *PLANT DEFENSIN 1.2* (*PDF1.2*) is a widely used marker gene for defense against necrotrophic pathogen attack and JA signaling. After *B. cinerea* inoculation, *PDF1.2* was induced in wildtype plants. Although this induction was not seen in *ckx3,5* and *snc1*, *PDF1.2* expression was higher after pathogen treatment in *s35* (Figure 9B). Surprisingly, JA levels in both *snc1* and *s35* were statistically higher than that of the other two genotypes, which could point to SA-JA synergism (Figure 9C). Though, it is possible that SA signaling in the *snc1* background is so high that the elevated JA content is masked by SA's suppression of downstream JA signaling. In conclusion, *s35* exhibits an altered state of immunity with increased resistance to pathogens of diverse lifestyles.

Transcriptome analysis of *s35* reveals an overabundance of redox- and nitrate-related gene expression

To gain insight into alterations of the transcriptome occurring within the reproductive tissue to yield the novel *s35* phenotype, we performed RNA sequencing analyses of inflorescences across genotypes. Three biological replicates per genotype were collected developmentally, when the primary shoot had at least one fully expanded flower (Stage 13+) present (Smyth et al., 1990). Inflorescences were dissected to Stage 12 and under, and cut from the stem, with between 15-18 inflorescences pooled per sample. mRNA was then extracted and subjected to quality control, library preparation, and sequencing. The Col-0 transcriptome was used as the control to identify differentially expressed genes (DEG). At a threshold of Benjamini-Hochberg's adjusted P value < 0.05, our analysis revealed 648 DEG (172 up and 476 down) in *ckx3,5*, 5767 DEG (3145 up and 2622 down) in *snc1*, and 4892 DEG (2575 up and 2317 down) in *s35* (Figure 10A). The high number of DEGs in the *snc1* and *s35* backgrounds in comparison to the *ckx3,5* double mutant underscores the strong influence of the

snc1 gain-of-function mutation on the global inflorescence transcriptome, likely due to the activation of several immune-related processes. DEGs, at a $\log_2$ fold change (FC) cutoff of |1|, were then analyzed between the three genotypes in comparison to wildtype plants (Figure 10B, 10C, and 10D), and Gene ontology (GO) analysis was used to characterize the DEGs from the gene comparison lists into biological process enrichment categories via the PANTHER 17.0 database (http://go.pantherdb.org/; Thomas et al., 2022). The GO terms relevant to the *ckx3,5* mutant mainly showed alterations to reproductive processes, most related to pollen tube growth. The GO terms "regulation of developmental growth" (Fold Enrichment (FE) = 14.34; False Discovery Rate (FDR) = 1.43E-05) and "regulation of reproductive process" (FE = 6.64; FDR = 2.93E-03) was shared between *ckx3,5* and *s35* (data not shown), potentially pointing to the increased meristematic activity in theses mutants. Unsurprisingly, *snc1* upregulated DEGs were largely categorized into defense-related GO terms (Figure 10E), many of which were shared with *s35* (Figure 10F). However, the GO term with the highest fold enrichment unique to the *snc1* background was "negative regulation of cytokinin-activated signaling pathway" (FE = 52.8; FDR = 0.0121), providing further evidence of SA's inhibitory effect on CK signaling (as seen in Figure 1).

Amongst the 192 uniquely upregulated DEGs in the *s35* background, only a single significant GO term was returned, "response to nitrate" (FE = 32.01; FDR = 0.0226). Within this category were several genes encoding CC-type glutaredoxins (*ROXY*s or *GRX*s). Glutaredoxins are thiol oxidoreductases, that bind to glutathione (GSH) and are likely involved in posttranslational modifications (Rouhier, Lemaire, & Jacquot, 2008). This gene family is known to play a role in nutrient sensing, specifically nitrate signal transduction (Jung, Ahn, & Schachtman, 2018). As CK levels have a positive correlation with nitrogen assimilation (Miyawaki et al., 2004; Takei et al., 2004) and have been identified as a long-range signal for nitrate availability (Sakakibara, 2006), we further analyzed this category. A total of 11 *ROXY* genes were significantly upregulated in *s35*, with $\log_2$ FC of up to 5.12 (Figure 11A), as well as

several nitrate transporters (*NRT*s and *NPF*s) and response genes (data not shown). To evaluate whether nitrate availability induced starbursting in out parental mutants, we fertilized plants at each watering with 24-8-16 nitrogen-phosphorus-potassium (NPK) macronutrient ratio. Heavy fertilization did not phenocopy the starburst in either *ckx3,5* or *snc1*, yet all four genotypes had improved growth (Figure 12). Moreover, NITRATE REDUCTASE 1 (NIA1) and NIA2 enzymes are responsible for the conversion of nitrate into nitrite or nitrous oxide (NO) (Lillo et al., 2004) and were recently shown to be expressed in the SAM (Olas et al., 2019). *snc1* and *s35* have increased expression of *NIA1* and *NIA2* in our data, suggesting that these mutants have altered nitrate metabolism, possibly contributing to changes in the reactive electrophilic species pool (data not shown).

ROS production happens during nitrate deprivation, which can lead to differential expression of *ROXY* genes in seedlings, where some are upregulated and others are downregulated (Jung, Ahn, & Schactman, 2018). This is likely due to the known function of GSH in redox buffering and ROS scavenging (Rouhier, Lemaire, & Jacquot, 2008). Moreover, salicylic acid treatment is associated with an oxidative burst in plant cells (Rao et al., 1997). To investigate if redox states play a role in reproductive growth alteration, we evaluated the expression of ROS-related genes in our dataset. *snc1* and *s35* showed several peroxidases (*PER*s) differentially expressed. PERs act as antioxidants by catalyzing the reduction of hydrogen peroxide (H_2O_2) to water. The induction of many of these genes in *snc1* and *s35* led us to examine H_2O_2 levels in inflorescences. A histochemical assay for H_2O_2 staining using 3, 3-diaminobenzidine (DAB) showed reduced levels in *snc1* compared to the rest of the genotypes (Figure 13), correlating with the increased PERs activity. However, this was not the case in *s35*, which had similar staining to wildtype. The *snc1* mutant has increased reactive species, including H_2O_2, when quantified in leaves and roots (Hao et al., 2011; Zhu et al., 2013; Guo et al., 2014; Wang et al., 2019). Our data suggest that ROS could be spatially sequestered throughout the plant in the *snc1* background, and the lack of this reactive species could impair

growth in reproductive tissue. Investigation into other reactive electrophilic species and antioxidants is needed to further characterize the redox status of each genotype.

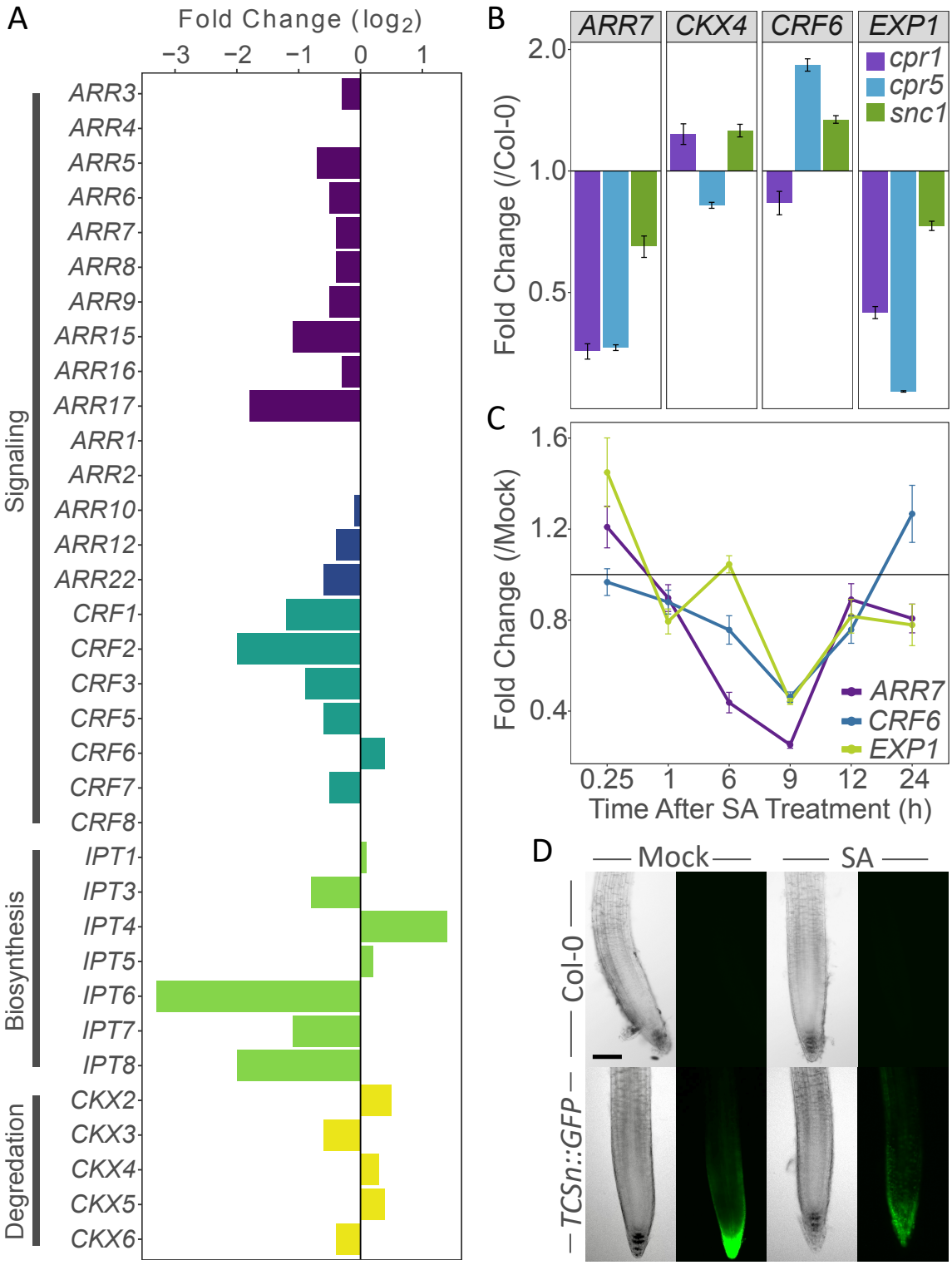

Figure 1: Salicylic acid has an inhibitory effect on cytokinin signaling. (**A**) Publicly available gene expression data of CK-regulated genes after SA treatment. Six-day-old wildtype seedings grown on plates were treated with 10 µM SA and tissue was collected 3 h after treatment.

Expression values are log_2-transformed and relative to the mock treatment. Data acquired and analyzed using the e-northern tool of the Bio-Analytic Resource for Arabidopsis Functional Genomics (http://bar.utoronto.ca; Toufighi et al., 2005). (**B**) CK-regulated gene expression of untreated mutants with increased SA biosynthesis/signaling: *constitutive expressor of PR genes 1* (*cpr1*), *constitutive expressor of PR genes 5* (*cpr5*), and *suppressor of npr1-1 constitutive 1* (*snc1*). RNA was extracted from untreated 3-week-old leaf tissue. *ARABIDOPSIS RESPONSE REGULATOR 7* (*ARR7*), *CYTOKININ OXIDASE 4* (*CKX4*), *CYTOKININ RESPONSE FACTOR 6* (*CRF6*), and *EXPANSIN 1* (*EXP1)* transcript levels were determined by qRT-PCR relative to wildtype plants. Error bars represent SE from three technical replicates and correspond to upper and lower limits of 95% confidence intervals. For better visualization, the axis is log_2-transformed. Data from one representative independent biological replicate are shown. At least three independent biological replicates of the experiment were conducted with similar results. (**C**) CK-regulated gene expression after 100 µM SA treatment over time. Wildtype seedlings were grown on 1X MS plates for 14 days. Seedlings were transferred to liquid MS and allowed to acclimate for 1 h on a shaker at 75 rpm under 120-150 µE light. SA, or solvent DMSO at 0.01%, were added to liquid culture. RNA was extracted from tissue collected at 0.25, 1, 6, 9, 12, and 24 h after hormone/mock treatment. Levels of *ARR7*, *CRF6*, and *EXP1* transcripts were determined by qRT-PCR relative to DMSO treatment. Error bars represent SE from three biological replicates and correspond to upper and lower limits of 95% confidence intervals. Data shown are three independent biological replicates pooled. (**D**) Fluorescence microscopy of 10 to 14-day-old Col-0 and transgenic *TCSn::GFP* roots treated with either mock or 50 µM SA. Representative images shown. Bright field (left); fluorescent imaging (right); n ≥ 20; scale bar = 100 µm.

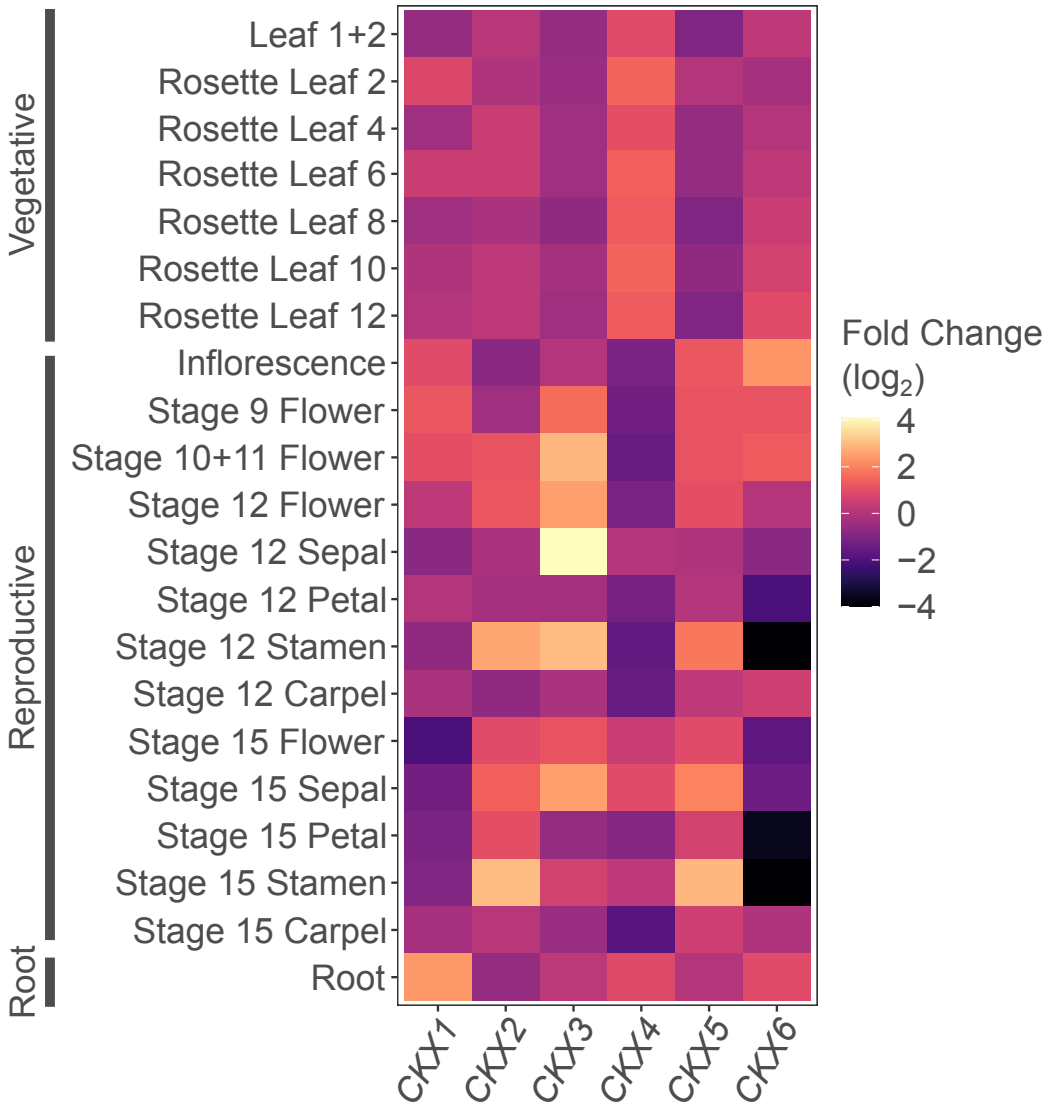

Figure 2: Tissue specificity of *CKX* gene expression. Publicly available gene expression data of six out of the seven *CKX* genes in different plant tissues. Expression values are log_2-transformed. Data acquired and analyzed using the e-northern tool of the Bio-Analytic Resource for Arabidopsis Functional Genomics (http://bar.utoronto.ca; Toufighi et al., 2005). Microarray gene expression normalized with robust multichip average (RMA) method.

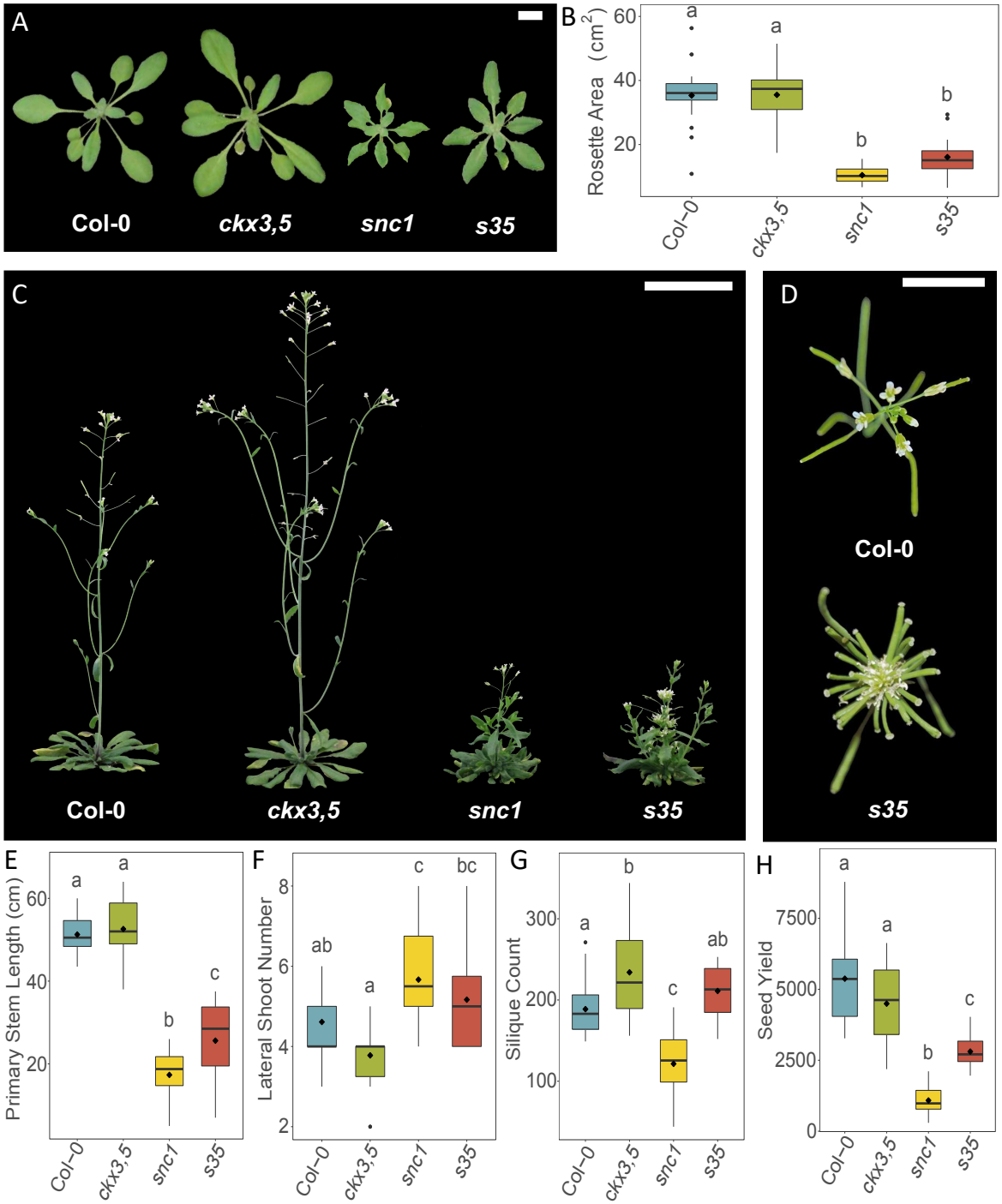

Figure 3: The *s35* triple mutant has a novel reproductive growth phenotype. (**A**) Representative vegetative growth phenotypes of each genotype 30 days after germination. Scale bar = 1 cm. (**B**) Rosette area of all genotypes 30 days after germination. (**C**) Representative flowering phenotypes of 50-day-old plants. Scale bar = 5 cm. (**D**) Representative inflorescences between wildtype Col-0 and *s35* at 8-weeks old. *s35* has a novel "starburst" inflorescence phenotype. Scale bar = 1 cm. (**E**) Stem length of the primary stem, (**F**) number of lateral shoots, and (**G**) average silique count of whole plants 10 weeks after germination. (**H**) Whole plant seed

yield collected 12 weeks after germination. For (**B**), (**E**), (**F**), (**G**), and (**H**), means labeled (◆) and statistical analysis performed using one-way ANOVA and significance differences labeled by letters. n = 18.

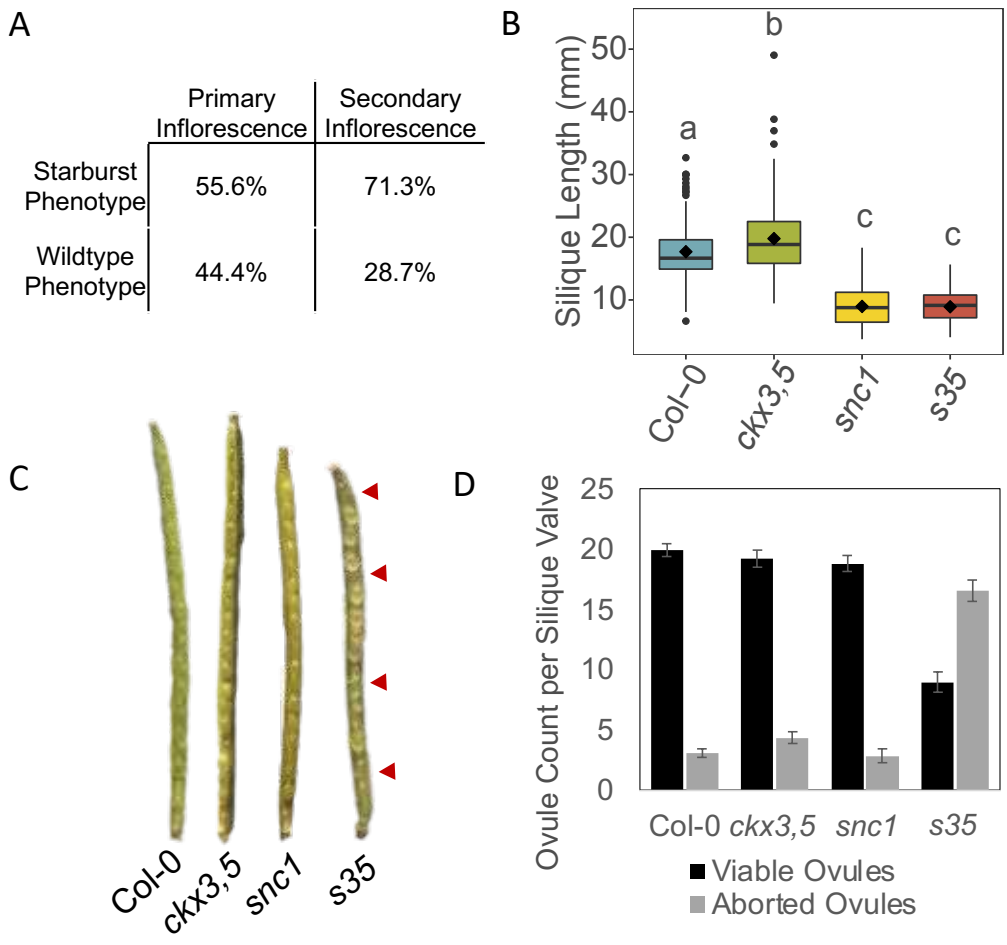

Figure 4: *s35* may have reduced seed yield due to ovule abortions and shorter siliques. (**A**) Penetrance of novel starburst phenotype of *s35* primary and secondary inflorescences. n = 18. (**B**) Silique length of each genotype. n > 100. Letters indicate differences at a $P < 0.05$ significance level using a one-way ANOVA analysis with a Tukey post-hoc correction. (**C**) Representatives of dissected siliques with aborted ovules indicated by red triangles (▲). (**D**) Viable versus aborted ovules per half silique. Siliques were dissected into two valves and ovules were counted. n ≥ 30 siliques.

Figure 5: *cpr1 ckx3 ckx5* (*c35*) has a starburst inflorescence phenotype similar to that of *s35*. The *c35* cross was confirmed via genotyping for homozygosity. Representative shown. Scale bar = 1 cm.

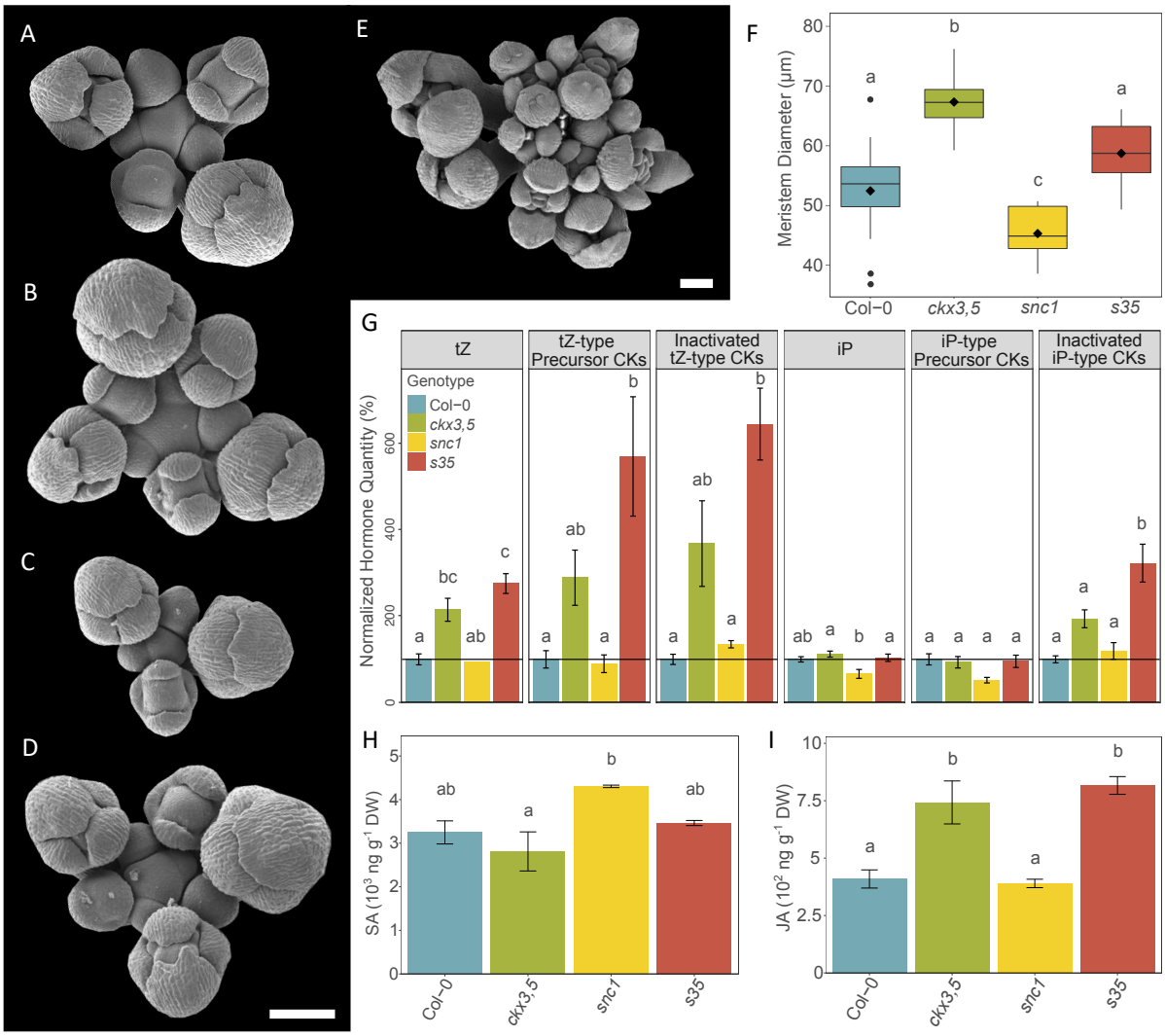

Figure 6: The *s35* triple mutant has altered inflorescence development due to changes in hormone balance. Representative electron scanning micrographs of hand-dissected primary shoot apical meristems of (**A**) Col-0, (**B**) *ckx3,5*, (**C**) *snc1*, and (**D**), (**E**) *s35*. Scale bars = 100 µM. (**F**) Diameter of hand-dissected primary shoot apical meristems. Means labeled (◆), and letters indicate differences at a $P < 0.05$ significance level using a one-way ANOVA analysis with a Tukey post-hoc correction. $n \geq 12$. Basal hormone quantification of different CK species normalized to Col-0: (**G**) tZ, tZ-type CK precursor, sum of tZR and tZRPs, inactivated tZ-type CK, sum of tZ7G, tZZ9G, tZOG, tZROG, and tZRPsOG, iP, iP-type CK precursor, sum of iPR and iPRPs, and inactivated iP-type CK, sum of iP7G and iP9G. See Table 3 for absolute values. (**H**) SA and (**I**) JA quantification of untreated inflorescence tissue. For (**G**), values represent percentage of wildtype CK species amount ± the percentage SEM of three technical replicates. For (**H**) and (**I**), values represent the mean ± the SEM of three technical replicates. For (**G**), (**H**), and (**I**), each replicate contained ≥ 30 inflorescences. Letters indicate differences at a $P < 0.05$ significance level using a one-way ANOVA analysis with a Tukey post-hoc correction.

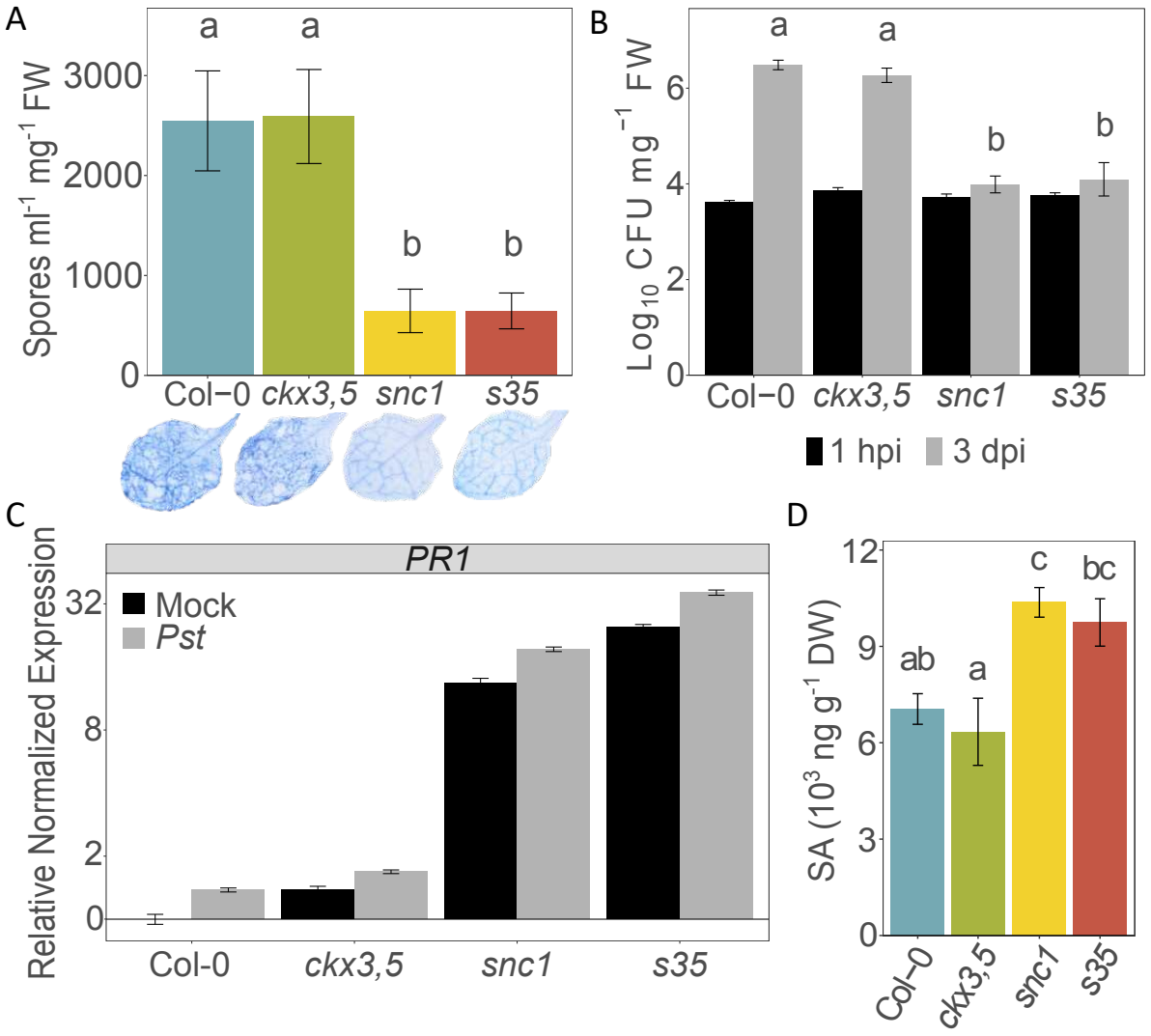

Figure 7: The *s35* triple mutant displays resistance against biotrophic pathogens. (**A**) *Hyaloperonospora arabidopsidis* Noco2 (*Hpa*) spore counts of each genotype at 3 dpi. Data shown are three independent biological replicates pooled. Below, representative leaves after trypan blue straining of *Hpa* hyphal/oospore growth. (**B**) Growth of *Pseudomonas syringae* pv. *tomato* DC3000 (*Pst*) at day 0 (T0) and at 3 dpi (T3). Data from one representative independent biological replicate are shown. At least three independent biological replicates of the experiment were conducted with similar results. (**C**) *PATHOGENESIS-RELATED 1* (*PR1*) expression 1 h after *Pst* inoculation (OD = 0.05). Levels of the indicated transcripts were determined by qRT-PCR relative to mock-treated wildtype plants and normalized to *UBIQUITIN 10* (*UBQ10*). Error bars represent SE from three biological replicates and correspond to upper and lower limits of 95% confidence intervals. For better visualization, the axis is $\log_2$-transformed. Data pooled from three independent biological replicates shown. (**D**) SA quantification of untreated 6-week-old leaf tissue. Values represent the mean ± the SE of three technical replicates. For (**A**), (**B**), and (**D**), letters indicate differences at a $P < 0.05$ significance level using a one-way ANOVA analysis with a Tukey post-hoc correction.

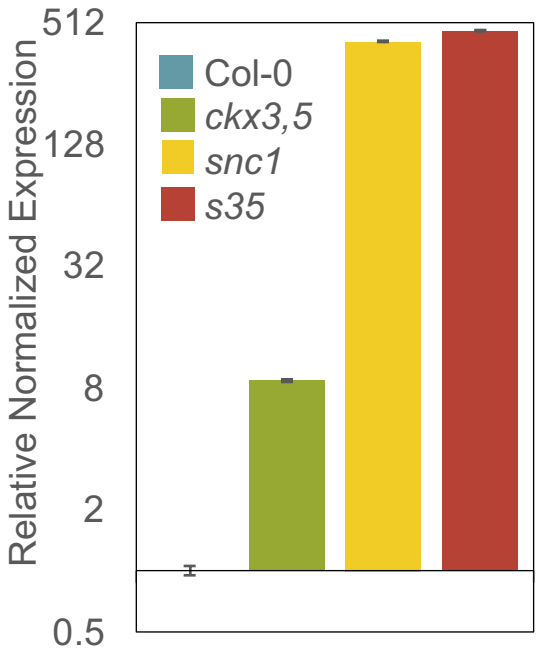

Figure 8: The *s35* triple mutant displays constitutive expression of *PR1*, similar to *snc1*. Basal levels of *PATHOGENESIS-RELATED 1* (*PR1*) transcripts were determined by qRT-PCR relative to wildtype plants and normalized to *UBIQUITIN 10* (*UBQ10*). Error bars represent SE from three biological replicates and correspond to upper and lower limits of 95% confidence intervals. For better visualization, the axis is $\log_2$-transformed. Data pooled from three independent biological replicates are shown.

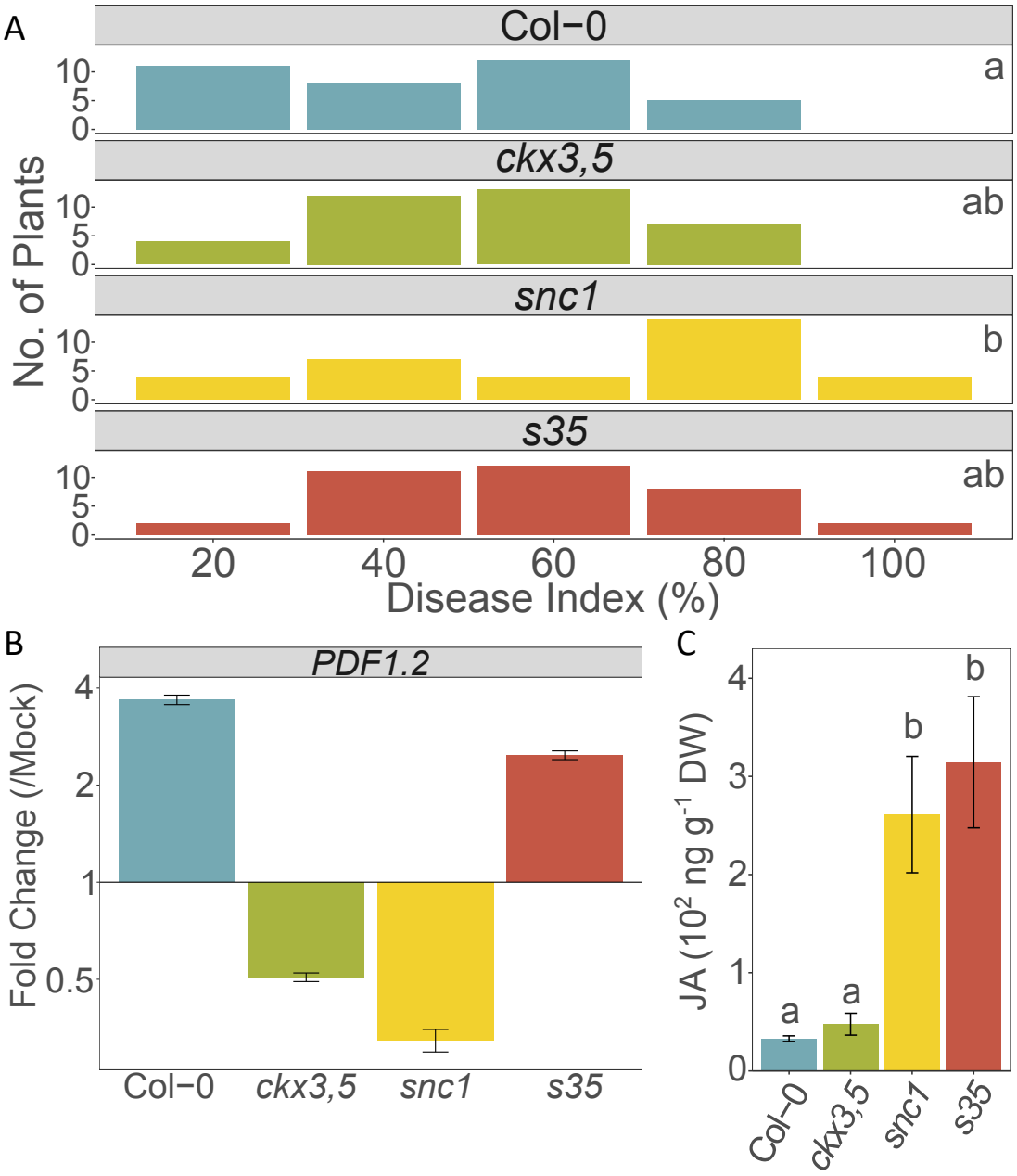

Figure 9: The *s35* triple mutant maintains resistance against necrotrophic pathogens. (**A**) Histograms of qualitative disease index of 6-week-old plants after *Botrytis cinerea* spray inoculation (0.5x10^4 spores/mL). Photographs of individual inoculated plants were taken at 96 hpi. Plants were categorized based on disease severity, where disease index represents percentage of rosette covered in necrotic lesions. Four independent biological replicates were conducted with similar results. Data from all four independent biological replicates were pooled. Letters indicate differences of disease index averages at a $P < 0.05$ significance level using a two-way ANOVA analysis with biological replicate as a blocking factor. (**B**) *PLANT DEFENSIN 1.2* (*PDF1.2*) gene expression 6 h after *B. cinerea* spray inoculation (0.5x10^4 spores/mL). Levels of the indicated transcripts were determined by qRT-PCR normalized to *UBIQUITIN 10* (*UBQ10*) and relative to mock-treated samples. Error bars represent SE from three technical replicates and correspond to

upper and lower limits of 95% confidence intervals. At least three independent biological replicates of the experiment were conducted with similar results. Data from one representative independent biological replicate are shown. For better visualization, the axis is log_2-transformed. (**C**) JA quantification of untreated 6-week-old leaf tissue. Values represent the mean ± the SE of three technical replicates. Letters indicate differences at a $P < 0.05$ significance level using a one-way ANOVA analysis with a Tukey post-hoc correction.

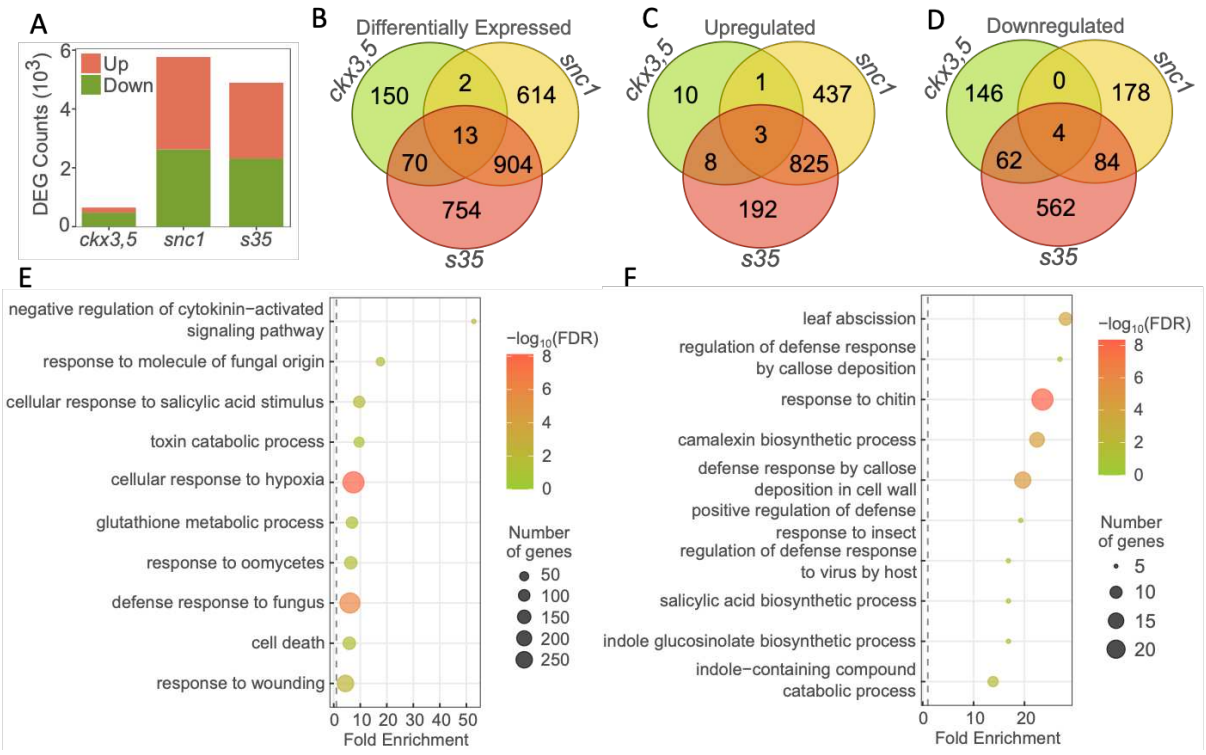

Figure 10: Transcriptome analysis of inflorescences reveals that the *snc1* gain-of-function mutation has a higher influence over genome-wide transcription in comparison to the *ckx* double knockout mutations. (**A**) Number of DEGs (up- and downregulated) of each genotype compared to the wildtype transcriptome of untreated inflorescence tissue. For the three biological replicates per genotype, each sample was collected developmentally, when the primary shoot had at least one fully expanded flower present (Stage 13+). DEG lists were compared amongst the mutant genotypes using Venn diagrams: (**B**) all differentially expressed genes, (**C**) up-regulated genes, and (**D**) downregulated genes. An arbitrary $\log_2$ fold change cutoff of 1 was used to reduce the DEG lists before comparison, and in analyses hereafter. (**E**) Gene Ontology (GO) term enrichment of uniquely up-regulated DEGs in the *snc1* background [437 genes from (**C**)]. (**F**) GO term enrichment of upregulated DEGs shared between *snc1* and *s35* [825 genes from (**C**)]. Terms with a significant fold enrichment of FE ≥ 12 shown. For (**E**) and (**F**), gene lists from the respective comparisons were analyzed for pathway enrichment using PANTHER 17.0 database (http://go.pantherdb.org/; Thomas et al., 2022). Only GO terms with an FDR corrected P value < 0.05 were considered significantly enriched.

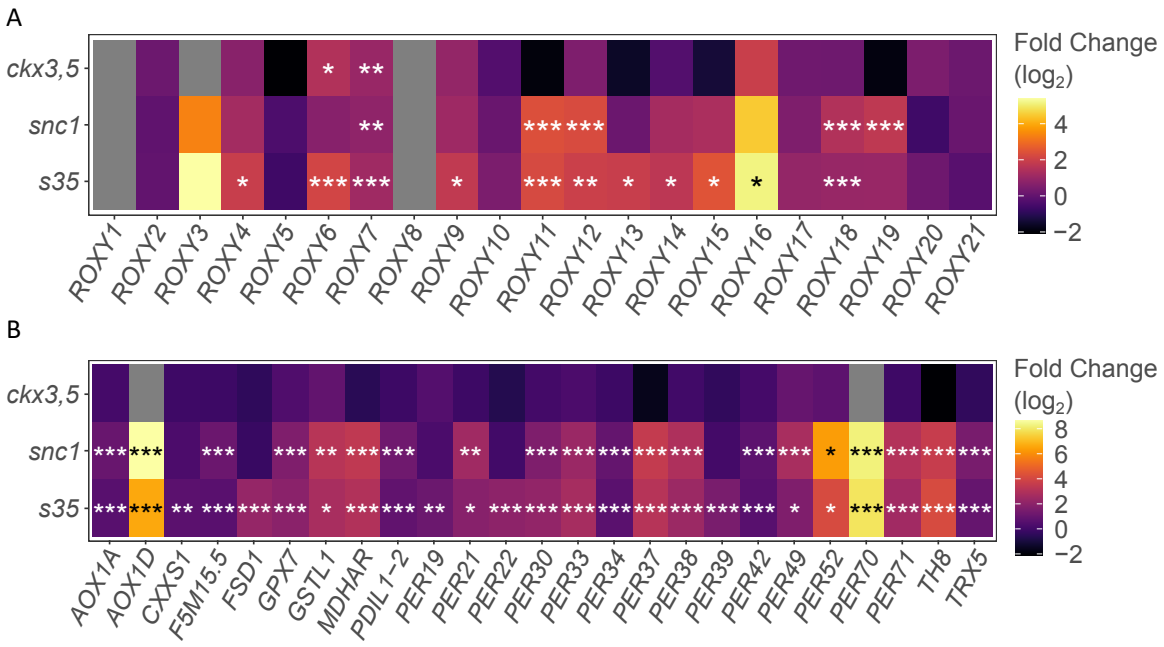

Figure 11: Transcriptome analysis of *s35* inflorescences reveals an overabundance of nitrate-related gene expression and altered redox gene regulation. (**A**) Gene expression of the CC-type glutaredoxin (*ROXY*) gene family in untreated inflorescences. (**B**) The most differentially upregulated ROS-related genes in the *s35* mutant as compared to its parental genotypes. Gene list was assembled from relevant literature and searched against the significantly DEGs of each genotype. For (**A**) and (**B**), statistically significant differences from wildtype inflorescences (FDR) are represented by asterisks (* = P value < 0.05, ** = P value < 0.01, *** = P value < 0.001).

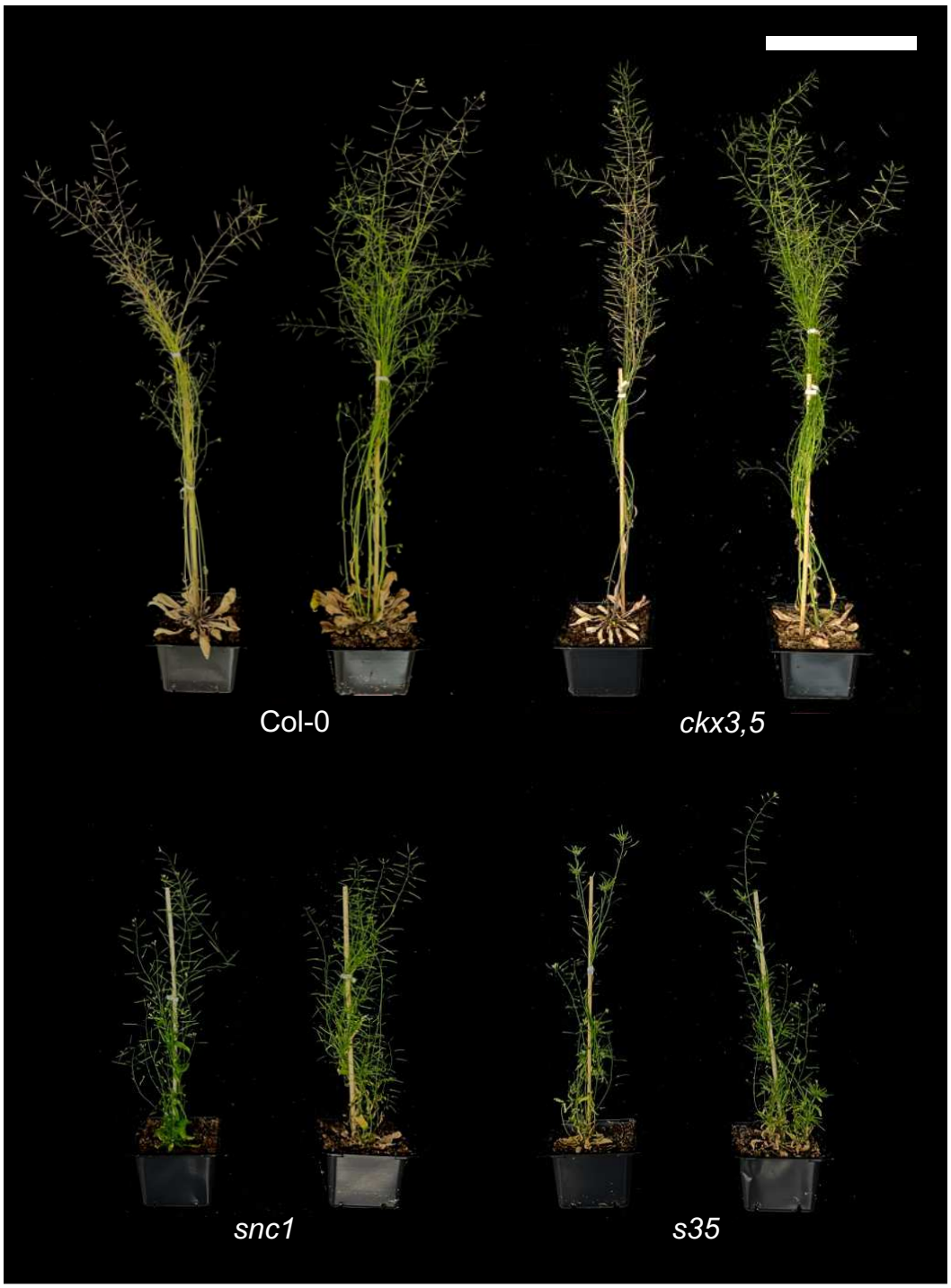

Figure 12: Treatment with fertilizer does not alter inflorescence morphology in *snc1* or *ckx3,5*. Col-0, *ckx3,5*, *snc1*, and *s35* watered with either water (left) or 1X Miracle-Gro Water Soluble All Purpose Plant Food (24-8-16) (right). Representatives of 10-week-old plants shown. n = 18. Scale bar = 15 cm.

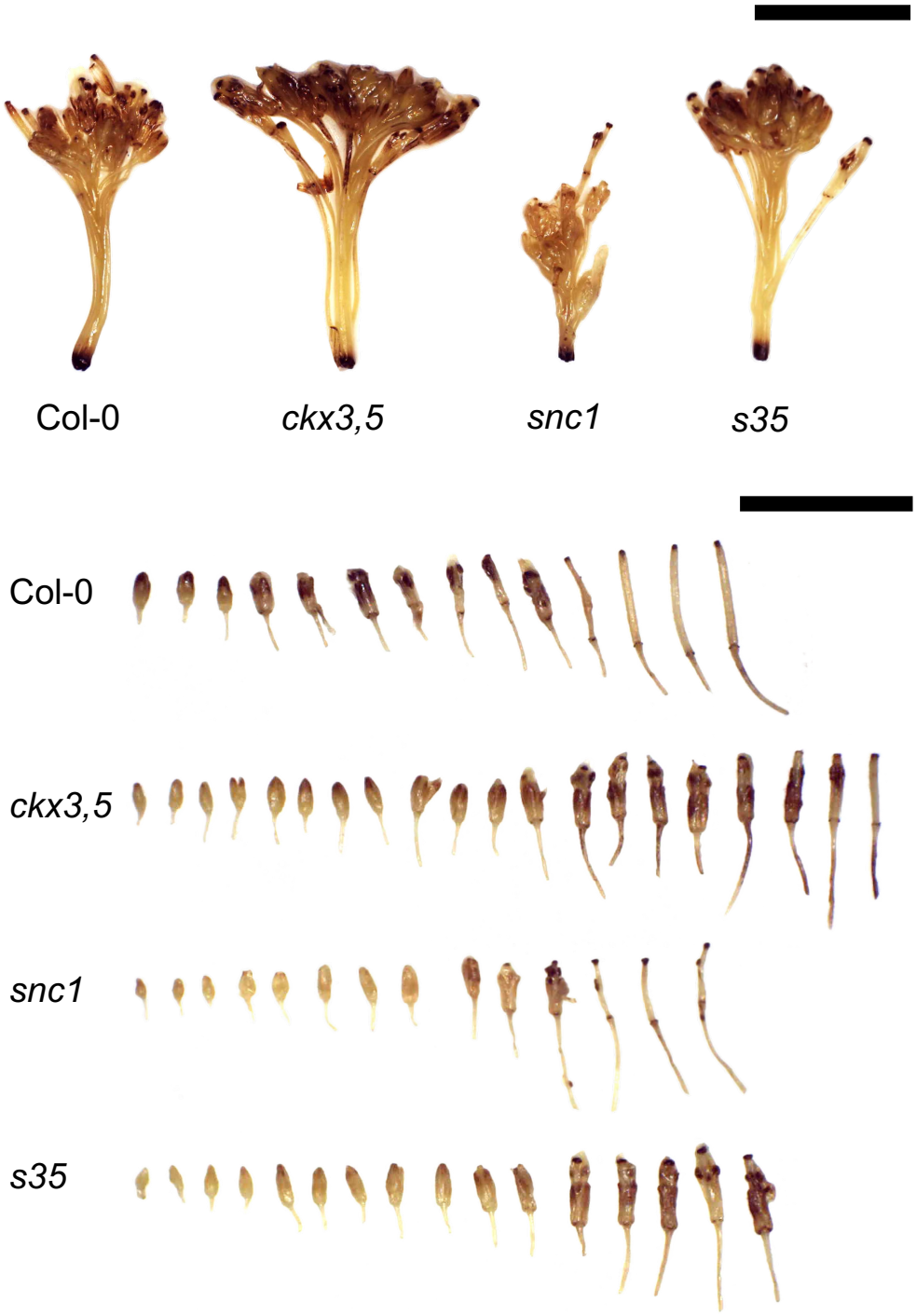

Figure 13: *snc1* has reduced H_2O_2 levels in inflorescences. Col-0, *ckx3,5*, *snc1*, and *s35* untreated inflorescences and dissected floral organs with hydrogen peroxide (H_2O_2) stained with 3, 3-diaminobenzidine (DAB). Representatives shown. Scale bars = 1 cm.

Table 1: Primers and restriction enzymes for mutant genotyping.

Table 1 — Primers for genotyping

Gene ID	Mutant	LP (5'→3')	RP (5'→3')	Restriction Enzyme	Products
AT5G56970	*ckx3-1*	TATCGAAAACGGACGGTGTAG	TGTCAACATTTTCTTCACAAAAAG	NA	WT: NA *ckx3-1*: ~700 bp
AT1G75450	*ckx5-1*	AATGGTATATTGTGATGACAGGTGAGA	TTGTTGCAGCAACGACCAACCGATAAT	NA	WT: NA *ckx5-1*: ~1000 bp
AT4G16890	*snc1*	TTGGAATACGTTTGCCATTCG	CCGTGGATCACAAGCCATAA	XBaI	WT: 847 bp *snc1*: 943 bp

Table 2: qRT-PCR quality control and gene specific primers for gene expression analysis.

Table 2 — qRT-PCR quality control and gene specific primers for gene expression analysis			
Gene ID	Gene Name	Forward (5'→3')	Reverse (5'→3')
AT1G19050	*ARABIDOPSIS RESPONSE REGULATOR 7* (*ARR7*)	ACTGTAGAGAGTGGAACTAGGGCT	AGTCCTGGCATTGAGTAATCCGTC
AT4G29740	*CYTOKININ OXIDASE/DEHYDROGENASE 4* (*CKX4*)	CACCCACAAGGGTGAAATGGTCTC	TGCGACTCTTGTTTGATCGGAGAG
AT3G61630	*CYTOKININ RESPONSE FACTOR 6* (*CRF6*)	TGGTTCAAGAGTGAAACGATAC	CTTTCCTCCTCCTTGTGCTTAC
AT1G69530	*EXPANSIN 1* (*EXP1*)	CAACGCATCGCTCAATACAG	CTCCGACGTTAGTGATCAGAAC
AT1G02450	*NIM1-INTERACTING 1* (*NIMIN1*)	GCACGGAAACGTAGACGAGAAG	GACCTTTCTCCGCCGTTAGATT
AT2G14610	*PATHOGENESIS-RELATED PROTEIN 1* (*PR1*)	ACAGTGCAATGGAGTTTGTGGTC	TACACCTCACTTTGGCACATCCGA
AT5G44420	*PLANT DEFENSIN 1.2* (*PDF 1.2*)	GCTTCCATCATCACCCTTATCTTC	ACATGGGACGTAACAGATACACTTGT
AT1G13320	*PROTEIN PHOSPHATASE 2A SUBUNIT A3* 1' (*PP2A* 1')	TAGATCGCTCGGAACTTGGAAA	CCTCACCAAAACTCAAATCACTCC
AT1G13320	*PROTEIN PHOSPHATASE 2A SUBUNIT A3* 3' (*PP2A* 3')	AACTAGGACGGATCTGGTGCCT	GCTATCCGAACTTCTGCCTCATTAT
AT1G13320	*PROTEIN PHOSPHATASE 2A SUBUNIT A3* 5' (*PP2A* 5')	AAATTTAACGTGGCCAAAATGATGC	GTTCTCCACAACCGCTTGGT
AT4G05320	*UBIQUITIN 10* (*UBQ10*)	CGTTAAGACGTTGACTGGGAAAACT	GCTTTCACGTTATCAATGGTGTCA

Table 3: The *s35* mutant has a unique CK species profile. Approximately 30 inflorescences per sample were harvested and pooled from 8-week-old plants. All samples were lyophilized. Three independent biological samples were harvested from each genotype. Data shown are pmol/g dry weight ± SD; n = 3. Asterisks (*) indicates percent SD over 50; peak annotations were rechecked. N.D. = not detected.

Table 3 — Cytokinin quantification of inflorescences				
Metabolite	Genotype			
	Col-0	*ckx3,5*	*snc1*	*s35*
tZ	0.79 ± 0.17	1.69 ± 0.36	0.74 ± N.D.	2.17 ± 0.31
tZR	16.65 ± 3.80	44.70 ± 16.43	13.28 ± 4.75	53.60 ± 10.65
tZRPs	9.75 ± 5.81*	31.73 ± 14.67	10.42 ± 4.84	97.15 ± 54.64*
iP	0.82 ± 0.09	0.92 ± 0.10	0.54 ± 0.15	0.85 ± 0.12
iPR	75.72 ± 24.38	62.38 ± 23.21	32.96 ± 8.72	34.94 ± 7.49
iPRPs	16.92 ± 5.14	24.06 ± 4.33	14.94 ± 4.01	53.52 ± 30.09*
cZ	1.26 ± 0.29	1.40 ± 0.44	1.00 ± 0.45	0.68 ± 0.27
cZR	270.33 ± 69.25	200.23 ± 68.40	131.70 ± 27.18	74.18 ± 25.16
cZRPs	26.46 ± 2.23	26.18 ± 2.46	22.36 ± 3.70	22.64 ± 0.65
DZ	N.D.	0.27 ± N.D.	0.12 ± N.D.	0.09 ± N.D.
DZR	0.42 ± N.D.	0.55 ± 0.20	0.41 ± 0.02	0.31 ± N.D.
DZRPs	0.32 ± N.D.	0.44 ± 0.13	0.41 ± 0.11	0.84 ± 0.54*
tZ7G	5.60 ± 1.18	19.60 ± 9.30	7.63 ± 1.05	36.16 ± 8.33
tZ9G	2.28 ± 0.51	9.93 ± 4.96	2.40 ± 0.34	14.73 ± 4.01
tZOG	0.83 ± 0.04	2.12 ± 0.81	2.07 ± 0.44	6.08 ± 0.68
cZOG	0.27 ± N.D.	0.59 ± 0.22	0.74 ± N.D.	1.14 ± N.D.
tZROG	0.60 ± 0.25	2.53 ± 0.86	0.50 ± 0.34	3.05 ± 1.14
cZROG	6.02 ± 0.87	6.12 ± 1.51	4.04 ± 0.27	3.85 ± 0.87
tZRPsOG	0.23 ± N.D.	0.45 ± 0.31*	0.17 ± N.D.	0.68 ± 0.37*
cZRPsOG	0.62 ± 0.19	0.68 ± 0.05	0.35 ± N.D.	0.39 ± 0.18
DZ9G	0.03 ± N.D.	0.04 ± N.D.	0.04 ± N.D.	0.06 ± N.D.
iP7G	23.58 ± 3.32	45.49 ± 8.47	28.02 ± 7.79	75.61 ± 17.90
iP9G	N.D.	0.29 ± 0.01	0.19 ± 0.08	0.64 ± 0.12

5. DISCUSSION

Phytohormone crosstalk should be considered a target for furthering crop advancements in the midst of ongoing global changes. In this research, we consider the crosstalk between two prominent phytohormones: cytokinin and salicylic acid. We determined that the balance between these hormones can be reconfigured via genetic mutation, resulting in the dampening of costs associated with immunity.

To best overcome environmental challenges, plants sequester resources, energy, and/or secondary metabolites toward a given response to secure survival, which can lead to a physiological shift away from other efforts. This tradeoff strategy is a dynamic fitness mechanism that has evolved in plants, as they cannot physically retreat from stressors. This is particularly the case during plant-microbe interactions, where growth is restricted, a phenomenon witnessed across plant species. As the growth-defense tradeoff is a limiting factor, crop breeding has previously maximized growth-related traits, sometimes at the expense of immunity (Strange & Scott, 2005).

Thus, ameliorating tradeoffs is not a novel aim for plant scientists, however specifically targeting phytohormone crosstalk as the means to achieve diminished tradeoffs has only recently been proposed (Albrecht & Argueso, 2017; Wasternack, 2017; Berry & Argueso, 2022). In order to adapt to environmental cues, plants utilize hormone signaling networks to fine-tune their physiological responses. For instance, a negative feedback regulatory module between signaling components of the gibberellin and SA pathways has been identified in Li et al., 2019b. During pathogen attack, DELLA proteins, which antagonize gibberellin-dependent growth, are accumulated. At the same time ENHANCED DISEASE SUSCEPTIBILITY 1 (EDS1), a SA immune regulator, facilitates defense responses. Direct interaction between DELLA proteins and EDS1 suppresses continual SA production. Together, the DELLA-EDS1 module determines the optimal growth-defense balance during pathogen infection, and the authors of Li et al.,

2019b suggest this crosstalk could be considered an engineering target for crop species optimization.

Defense in *s35*

The crosstalk between the CK and SA pathways has been previously identified in Arabidopsis and other species (Choi et al., 2010; Argueso et al., 2012; Jiang et al., 2013), mostly by defining the positive influence of CK on SA signaling upon pathogen perception. Our data further elucidate the negative effect of SA on CK signaling that had been previously indicated (Argueso et al., 2012) and shows that this negative effect also exists in the context of constitutive immune activation. This may well be a part of the mechanisms behind the growth-defense tradeoff to bolster the antagonism between these pathways. Plants that are under active attack from biotrophic pathogens respond with induction of SA-dependent defense responses. Possibly to conserve or reallocate resources or energy, elevated SA levels and signaling could in turn dampen CK growth-related processes. Yet, we hypothesized that growth and defense could be uncoupled by modifying these two hormone pathways. Instead of targeting specific transcription factors or protein-protein interactions, we opted to re-engineer the CK-SA crosstalk via increasing basal hormone levels in the *s35* mutant.

The snc1 gain-of-function mutant used in this study is highly resistant against biotrophic pathogens, like *Pst* and *Hpa*, (Li et al., 2001) and these results were confirmed in our work (Figure 7). Resistance to a biotrophic pathogen is usually accompanied by SA accumulation, which can antagonize defense responses to necrotrophs mediated by JA (Spoel, Johnson, & Dong, 2007; Pieterse et al., 2012), hindering broad spectrum resistance. Yet, *s35* is less susceptible to the necrotrophic fungus, *B. cinerea*, when compared to *snc1* (Figure 9A), and thus represents a mutant combination that provides broad resistance to biotrophs and necrotrophs. Recently, a function for CKs in immunity against necrotrophic pathogens was observed in tomato, where application of micromolar amounts of CKs had a protective effect

against *B. cinerea* and proper JA signaling was needed for this response (Gupta et al., 2020). Thus, similarly to what happens with responses to biotrophic pathogens, increased CK content in the *s35* triple mutant amplifies JA-regulated defense responses to necrotrophic pathogens upon pathogen infection. Moreover, these results suggest that, even though the effects of the *ckx3* and *ckx5* mutations are largely localized in reproductive tissue (Figure 2), CK can partially mediate necrotrophic and biotrophic defense responses in other parts of the plant.

Growth in *s35*

We observed significant morphological aberrations in the *s35* mutant. Namely, the reproductive cost of immunity characteristic of the *snc1* phenotype was partially rescued by the *ckx3,5* mutations. Although *s35* retained dwarfed vegetative growth, the reproductive outcome was comparable to wildtype, in terms of seed pods, but not seed yield. If mimicked in crop species, this could be an attractive phenotype to farmers of fruit crops. Smaller plants would allow for more individuals to be grown per plot. Although this mutation combination yields similar fruiting capacity to wildtype, the lack of seed production is problematic. Yet, it is possible that this reduced seed set may be offset by the significant increase in resistance to a broad spectrum of pathogens, achieving a net harvest increase. Application of this work in crops would be a large undertaking, although research in integrating mutations in *CKX* genes in oilseed rape led to enhanced reproductive growth compared to wildtype, with increased floral organs and seed weight per plant in field-grown conditions (Schwarz et al., 2020). There are several examples of highly resistant crop cultivars, yet many exhibit a growth tradeoff (reviewed in Brown, 2002). Taken together, our results provide evidence of uncoupled growth and defense that could motivate the CK-SA crosstalk as targets for crop improvement.

Normative growth patterning of meristematic tissue is under tight regulation by phytohormone crosstalk. A positive feedback loop between the WUSCHEL (WUS) transcription factor and the CLAVATA (CLV) signaling peptide maintain regions of the meristem and are

influenced by CK and auxin (Su, Liu, & Zhang, 2011; Azizi et al., 2015). CK promotes *WUS* expression to maintain the stem cell niche (Gordon et al., 2009). To increase CK levels, in turn, WUS directly inhibits type-A *ARR*s, repressing the CK pathway negative regulation (Leibfried et al., 2005; Zhao et al., 2010). Restricting the stem cell domain, CLV antagonizes WUS, but is itself repressed by CK (Gordon et al., 2009). Loss of auxin accumulation in this region induces type-A *ARR* expression, suggesting that auxin inhibits CK signaling during normal development (Zhao et al., 2010). Mutations in *ARABIDOPSIS HISTIDINE PHOSPHOTRANSFER PROTEIN 6* (*AHP6*), a CK signal inhibitor, yielded increased SAMs (Besnard, Rozier, & Vernoux, 2014). Therefore, modification of the maintenance mechanisms controlling reproductive growth, including phytohormone crosstalk, can lead to novel phenotypic outcomes.

Recently, SA has been identified as influencing root apical meristem (RAM) regulation in a concentration dependent manner. Low concentrations of SA applied to seedlings promote advantageous root growth, while high concentrations halt RAM development (Pasternak et al., 2019). Notably, in our work we provide evidence for a link between endogenous SA levels and SAM development. *snc1* has high accumulation of SA in inflorescence tissue (Figure 6H) and smaller meristems (Figure 6F), suggesting SA antagonizes SAM growth. Moreover, *s35* not only has increased meristematic activity similar to *ckx3,5*, but also altered silique phyllotaxy and floral organ morphology (Figure 6E). This implicates SA or its downstream signaling in SAM developmental regulation. To our knowledge, this is the first time SA has been implicated in SAM regulation. Future experimentation is necessary to identify the mechanisms behind this.

Possible molecular mechanisms mediating the uncoupling of growth and defense in the *s35* triple mutant

Our transcriptomics data suggests that the altered regulation of the SAM in the *s35* mutant is related to nitrate responsive genes. As described, a single gene family was highlighted in our GO analysis of *s35*: the CC-type *ROXY* glutaredoxin subgroup. ROXYs

catalyze the reduction of disulfide bonds of target proteins (Rouhier, Gelhaye, & Jacquot, 2004). Several of these genes have been mutated in Arabidopsis in attempt to understand their mechanistic function and have been shown to play a role in development, nutrient sensing, and stress responses (reviewed in Gutsche et al, 2015). In Arabidopsis, nitrogen starvation results in differential expression of the CC-type glutaredoxins (Jung, Ahn, & Schachtman, 2018). Apoplastic ROS is increased during nutrient deprivation and can, likewise, cause alteration of *ROXY* gene expression. These findings, uncovered in Jung, Ahn, & Schachtman, 2018, suggest ROXYs and ROS act in tandem as part of nutrient sensing signal transduction throughout the plant.

Furthermore, some *ROXY* genes, specifically *ROXY1*, *ROXY2*, and *ROXY4*, impact the classic ABCDE (formerly ABC) homeotic gene patterning of floral organ differentiation and initiation (Rijpkema et al., 2010). Each class of gene, of which most are MADS-box transcription factors, function to initiate or suppress organs of the four floral whorls. One of the most well characterized is the *roxy1* mutant, which exhibits deformed floral organs. It was found that ROXY1 acts to repress the homeotic class C genes during the development of the first two whorls (Jung, Ahn, & Schachtman, 2018). Although this gene is not differentially regulated in *s35* inflorescence tissue, it offers evidence of ROXY function in reproductive organs.

Recently, a study in maize determined that ZmGRXs act in SAM development, target TGA transcription factors, and influence redox state of the stem cell niche. Yang et al., 2021a observed significant defects to ear development in *grx* double and triple knockout mutants, yielding significantly less kernels than wildtype. Genetic analysis revealed that the *MALE STERILE CONVERTED ANTHER 1* (*ZmMSCA1*) gene acts redundantly with *ZmGRX2* and *ZmGRX5*. To modulate meristem growth, these proteins target FASCIATED EAR 4 (ZmFEA4), a TGA transcription factor that suppresses ear development, for redox modification. In the *grx* triple mutant, ZmFEA4 is in an oxidized dimer state, allowing for enhanced activity in repressing normative meristem development (Yang et al., 2021a).

As NPR1 forms a transcriptional complex with TGAs in redox-dependent reaction during SA signaling, ROXY modifications could be significant in *snc1* and *s35* mutants. In Arabidopsis, there are ten *TGA* genes, grouped into five different clades (Gatz, 2013). NPR1 has been shown to interact with TGA1, TGA3, and TGA6, but it is also suspected that NPR1 may act in the same pathway as that of clade-I TGAs (TGA1/4) (Zhang et al., 2003; Kesarwani et al., 2007; Saleh et al., 2015). Besides Yang et al., 2021a, other research has found ROXY-TGA interactions in Arabidopsis. ROXY 9 has been suggested to repress clade-I TGA activity in response to nitrogen assimilation for transcription of nitrate transporters (Alvarez et al., 2014). One of the ways ROXYs can modify floral whorl development is through interaction with the TGA transcription factor, PERIANTHIA (PAN). PAN ensures floral primordia are initiated in the correct position around the floral meristem of the first three whorls (Running & Meyerowitz, 1996) and is proposed to be post-translationally modified by ROXY1 (Xing & Zachgo, 2008; Li et al., 2009). Although there is much indirect evidence, as of 2019, it is still not fully established that ROXYs directly reduce TGA active site cysteine residues (Li et al., 2019a).

*ROXY*s, particularly *ROXY18* and *ROXY19*, are responsive to pathogen attack and may hinder defense responses. Both of these genes are induced by the presence of a pathogen and SA treatment (Ndamukong et al., 2007; Laporte et al., 2011). The *roxy18* knockout mutant is less susceptible to *B. cinerea*, suggesting *ROXY18* to be a necrotrophic susceptibility gene (Laporte et al., 2011). Moreover, JA treatment reduced *ROXY18* transcription, lending further evidence that it may facilitate *B. cinerea* colonization. On the other hand, *ROXY19* is induced by JA. Though, ectopic expression of *ROXY19* increased susceptibility to *B. cinerea* and repressed transcription of *PDF1.2* (Ndamukong et al., 2007; Lai et al., 2014). Clade-II TGA activity is also susceptible to modification by over expression of *ROXY19* (Ndamukong et al., 2007; Zander et al., 2012). Notably, both *snc1* and *s35* have significantly upregulated *ROXY18* expression in our transcriptome data (Figure 11), but only *snc1* has significant induction of *ROXY19* ($\log_2$ FC = 1.73, P = 0.0011; data not shown). As they appear to function in SA-JA mutual antagonism, the

induction of these ROXYs may contribute to the susceptibility phenotype of the *snc1* and *s35* mutants to *B. cinerea* challenge (Figure 9A), and the results of our JA quantification and gene expression (Figure 9B and 9C).

Alternatively, a link between CK and glutaredoxins has also been proposed. Semi-dwarfed plants with reduced grain set are observed if rice *OsGRX6* is overexpressed (El-Kereamy et al., 2015). This gene is known to be induced by SA and other external stimuli (Garg et al., 2010). Further characterization revealed that CK content, biosynthesis, and signaling were significantly higher with *OsGRX6* overexpression, as well as increased nitrogen content (El-Kereamy et al., 2015). Yet, it was not studied whether the increased nitrogen content was due to the high CK biosynthesis/signaling, or vis versa. Previous research has associated increased CK levels with deleterious growth impacts in rice seen as in Sakamoto et al., 2006. Most recently, a link between nitrogen sensing and CK signaling was proposed to be mediated by ROXY6 and/or ROXY9, referred to in this work as CEP DOWNSTREAM 1 (CEPD1) and CEPD2, respectively. C-TERMINALLY ENCODED PEPTIDE (CEP) is a novel peptide hormone acting in signal transduction during environmental fluctuations, including nitrate status (Taleski, Imin, & Djordjevic, 2018). CEPDs coordinate crosstalk between CEP and CK for ideal regulation of root growth in response to nitrogen acquisition (Taleski et al., 2022). Together, ROXYs have been implied to have a synchronizing function in hormone signaling and stimuli perception. Thus, it is possible that the increased CK-SA content and upregulation of *ROXY* genes in the *s35* mutant contribute to changes in nitrogen concentration in reproductive tissue and allow for morphological alterations. Landrein et al., 2017 found that SAM size is tightly regulated by nitrate availability at the roots and subsequently systemic CK signaling. Nitrogen levels would need to be quantified and the sufficiency and necessity of the nitrogen response to CK-ROXY relationship tested. Alternatively, if nitrogen concentrations are not altered in our mutants, the perception of nitrogen status could be different, in which we would have to further analyze nutrient signal transduction. We tested nitrogen response by increasing nitrogen availability

through continuous fertilization of the soil. This did not cause *ckx3,5* or *snc1* to starburst, nor did *s35* plants revert to wildtype inflorescence morphology (Figure 12). Instead, each genotype, wildtype included, grew noticeably larger when watered with fertilizer in comparison to just tap water, though not quantified in our experiment. Because increasing nitrogen availability did not phenocopy *s35* in the *snc1* background, it is possible that nitrogen assimilation, translocation, or metabolism is not the mechanism behind the increased reproductive fitness of *s35* plants. Alternatively, different levels of fertilization may be required for the development of the starburst phenotype.

As ROXYs function to maintain redox status of the cell during development and immunity, so too do reactive electrophilic species, ROS and reactive nitrogen species (RNS), which act as key signaling molecules in many plant physiological processes. The role ROS and RNS play in both biotic and abiotic stress has been well characterized (del Río, 2015; Sachdev et al., 2021; Khan et al., 2023). Yet, ROS's function in stem cell maintenance was only recently found (Zeng et al., 2017). Spatial patterning of different species is important for normal meristem development: actively dividing cells in the central zone have high accumulation of superoxide, while differentiating cells in the peripheral zones accumulate H_2O_2. These ROS target *WUS*, a homeobox gene necessary for preserving stem cells in an undifferentiated state, for differential expression (Zeng et al., 2017). In rice, a mutant in *APICAL SPIKELET ABORTION* (*OsASA*) is defective in spikelet development and has both H_2O_2 and SA overaccumulation (Zhou et al., 2021).

Moreover, RNS, specifically the gaseous radical nitric oxide (NO), has also been shown to play a role in meristem maintenance. A mutant of *NO ASSOCIATED 1* (*NOA1*) is NO deficient and has smaller inflorescences with less floral organs compared to wildtype (Shen et al., 2013). Using florescent probes, NO synthesis was found in specific cell types of floral organ fate, insinuating there is a spatial patterning imperative for typical inflorescence development, much like ROS (Seligman et al., 2008). The expression of a CK-responsive cell cycle gene,

CYCLIN D3;1 (*CYCD3;1*), was also impaired in *noa1*. Shen et al., 2013 theorized that NO acts downstream CK to regulate cell division and expansion through induction of *CYCD3;1*. However, research on the relationship between NO and CK is inconsistent. Romanov et al., 2008 did not find a link between NO and primary CK signaling. When a β-glucuronidase (*GUS*) reporter gene was driven under type-A *ARR5* promoter in transgenic Arabidopsis, NO donors did not activate *GUS* transcription, nor did NO scavengers inhibit *ARR5* after CK treatment (Romanov et al., 2008). Additionally, tZ treatment reduced high endogenous NO levels in the *nitric oxide overexpression 1* (*nox1*) mutant, suggesting that CK suppresses NO through direct chemical interaction (Liu et al., 2013). Hence, this relationship requires further scrutiny.

NO is clearly important during immune activation as a secondary messenger and may work in conjunction with ROS (reviewed in Bellin et al., 2013). At high cellular concentrations, NO perpetuates *S*-nitrosylation of target proteins, where NO is covalently bonded to cysteine residues in the active site (Lindermayr & Durner, 2009). In fact, NO can react with GSH, resulting in *S*-nitrosoglutathione or GSNO. Catabolism of GSNO by GSNO reductase (GSNOR) oxidized GSH and ammonia (NH_3) (Rustérucci et al., 2007). Disrupting GSNOR accumulation in Arabidopsis decreased susceptibility to *Hpa* attack (Rustérucci et al., 2007, Hong et al., 2008). As our transcriptomic analysis revealed *snc1* has significant enrichment of genes representing "glutathione metabolic process" (Figure 10E), this could contribute to its substantial resistance towards *Hpa* (Figure 7A). Moreover, SA induces enzymatic pathways to contribute to increased NO production (Zottini et al., 2007). During SA signaling, NPR1 is susceptible to oxidation by NO. Though, it is unclear whether *S*-nitrosylation of NPR1 promotes its oligermized form in the cytosol (Tada et al., 2008) or its translocation to the nucleus (Lindermayr et al., 2010). As NO is also induced by JA and wounding herbivory (Huang et al., 2004), it is suggested that NO works at the intersection of SA-JA crosstalk by Mur et al., 2013.

In conjunction with NO, temperature and nitrogen availability influence immune status. Characterized in Wang et al., 2013, NUDIX HYDROLASE HOMOLOG 6 (NUDT6) and NUDT7

act redundantly to suppress EDS1-mediated defense and are proposed to act upstream of *SNC1*. In high nitrate conditions (low ammonium/nitrate ratio), nitrite and NO accumulate in the double knockout *nudt6,7*, which amplify autoimmunity. Remarkably, *nudt6,7* plants have a very similar inflorescence phenotype to *s35* starbursts, in which successive floral organs are compressed at the shoot apex. Although this phenotype only appears when the plants undergo a temperature transition from high heat (28°C) to regular temperature (22°C). Crossing *nudt6,7* to loss-of-function *snc1-11* further sensitized the plant to temperature, as the abnormal inflorescence phenotype would be present in temperature shifts from 22°C to 19°C (Wang et al., 2013). The gain-of-function *snc1* mutant used in our work is prone to temperature sensitivity; at high temperatures it loses its dwarfed vegetative phenotype and autoimmunity (Zhu et al., 2010; Gou & Hua, 2012; Huot et al., 2014). In our transcriptomic analysis, both *NUDT6* and *NUDT7* are upregulated in *snc1* and *s35* (data not shown), suggesting these may be key players in nitrate sensing, NO signaling, and meristem maintenance during autoimmunity. Though, further experimentation is necessary to fully grasp *NUDT*s mechanistic contributions to our temperature-insensitive starburst phenotype.

In turn, NO produced from nitrate assimilation inhibits GSNOR by nitrosylation, preventing the scavenging of GSNO and thus could be modulated due to the enhanced nitrate response in the *s35* background. *NOA1* is not differently regulated in *ckx3,5* or *s35*, but is significantly downregulated in *snc1* ($\log_2$ FC = -0.274, P = 0.0316; data not shown). *snc1* and *s35* have increased expression of *NIA1* and *NIA2* in our data (data not shown), suggesting that these mutants have altered nitrate metabolism, possibly contributing to changes in the reactive electrophilic species pool.

Conclusions & future directions

We propose that the novel hormonal balance within the *s35* mutant could change the plant's perception of nitrate availability, and subsequent metabolism, causing a cascade of

signaling modifications through redox reactions and *ROXY* genes, ultimately resulting in overactive meristem activity and organogenesis (Figure 14). We hypothesize that the *ckx3,5* mutations lead to alteration of nitrate sensing and/or translocation, and the *snc1* mutation results in cellular redox imbalance. When combined in the *s35* mutant, the impaired growth due to constitutive defense activation is partially rescued by increased CK and its downstream effects.

Future experimentation is necessary to fully resolve this hypothesis and determine the mechanistic components regulating the *s35* starburst phenotype. Although we did not glean many answers from our fertilization experiment, addressing nitrate signal transduction throughout the plant and concentrations of molecules involved in nitrate metabolism would give insight to any misregulation occurring. Furthermore, quantification of redox species would allow for correlation between redox status and meristem activity. Similarly, phenocopy experiments with ROS/RNS inhibitors and donors would be informative in identifying necessity and sufficiency. The insights uncovered here and in the future progression of this project will allow for a more complete understanding of the impact CK and SA have on growth and immunity, and ultimately, be valuable for engineering crop species with diminished tradeoffs.

As it is progressively evident that breeding programs will need to adapt their practices for future sustainability, our research facilitates new avenues to be explored in crop species by exploiting the natural signaling molecules governing plant fitness and survival. While other studies uncovered instances of uncoupled growth and immunity, we hypothesized that hormone crosstalk is the key to achieving this. By increasing hormone content in the model plant Arabidopsis, the *s35* mutant we characterized here, validates our hypothesis and allows for evaluation of the underlying mechanisms behind the CK-SA crosstalk, mediating synergistic growth and defense. Using the principles behind translational science, we hope these findings can be applied to engineering improved crop species by precision genome editing to meet the near-future's high demand and environmental changes.

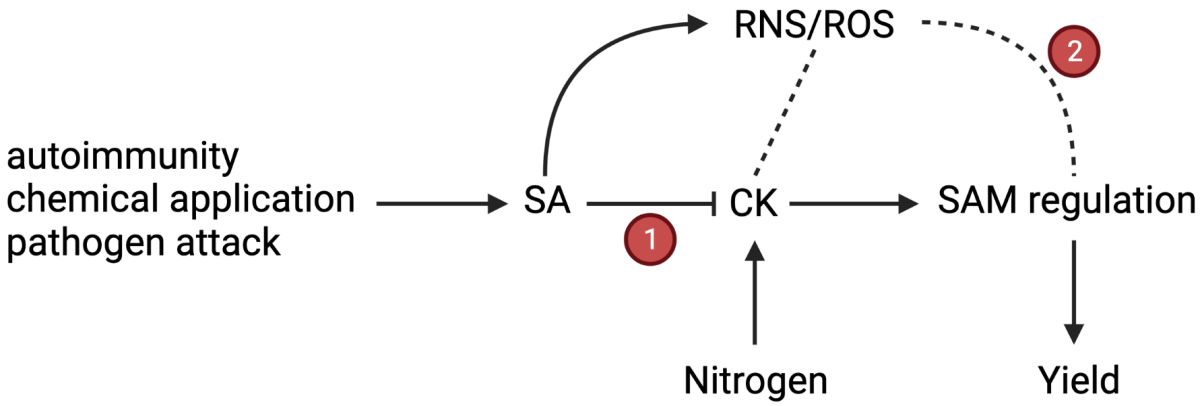

Figure 14: Proposed model of SAM regulation in relation to the CK-SA crosstalk. SA is activated by either genetic mutations conferring autoimmunity, exogenous application of SA or related chemicals, or pathogen attack. During defense, SA triggers the production of reactive nitrogen species (RNS) and reactive oxygen species (ROS), leading to impaired growth and reproductive yield. CK levels have a positive correlation with nitrogen assimilation and have been proposed as a long-range signal for nitrate availability. CK maintains the stem cell niche in the SAM and promotes fitness. (**1**) Supported by our data, SA transcriptionally represses CK signaling. (**2**) Redox status modulates SAM activity directly or oxidoreductive modification of target proteins. Dashed line represents unknown relationship.

REFERENCES

Albrecht, T., & Argueso, C. T. (2016). Should I fight or should I grow now? The role of cytokinins in plant growth and immunity and in the growth–defence trade-off. *Annals of Botany*, mcw211. https://doi.org/10.1093/aob/mcw211

Allen, L. H., Zhang, L., Boote, K. J., & Hauser, B. A. (2018). Elevated temperature intensity, timing, and duration of exposure affect soybean internode elongation, mainstem node number, and pod number per plant. *The Crop Journal*, *6*(2), 148–161. https://doi.org/10.1016/j.cj.2017.10.005

Aloni, R., Langhans, M., Aloni, E., Dreieicher, E., & Ullrich, C. I. (2005). Root-synthesized cytokinin in Arabidopsis is distributed in the shoot by the transpiration stream. *Journal of Experimental Botany*, *56*(416), 1535–1544. https://doi.org/10.1093/jxb/eri148

Altmann, M., Altmann, S., Rodriguez, P. A., Weller, B., Elorduy Vergara, L., Palme, J., Marín-de la Rosa, N., Sauer, M., Wenig, M., Villaécija-Aguilar, J. A., Sales, J., Lin, C.-W., Pandiarajan, R., Young, V., Strobel, A., Gross, L., Carbonnel, S., Kugler, K. G., Garcia-Molina, A., … Falter-Braun, P. (2020). Extensive signal integration by the phytohormone protein network. *Nature*, *583*(7815), 271–276. https://doi.org/10.1038/s41586-020-2460-0

Alvarez, J. M., Riveras, E., Vidal, E. A., Gras, D. E., Contreras-López, O., Tamayo, K. P., Aceituno, F., Gómez, I., Ruffel, S., Lejay, L., Jordana, X., & Gutiérrez, R. A. (2014). Systems approach identifies TGA1 and TGA4 transcription factors as important regulatory components of the nitrate response of *Arabidopsis thaliana* roots. *The Plant Journal*, *80*(1), 1–13. https://doi.org/10.1111/tpj.12618

Apel, K., & Hirt, H. (2004). REACTIVE OXYGEN SPECIES: Metabolism, Oxidative Stress, and Signal Transduction. *Annual Review of Plant Biology*, *55*(1), 373–399. https://doi.org/10.1146/annurev.arplant.55.031903.141701

Argueso, C. T., Ferreira, F. J., Epple, P., To, J. P. C., Hutchison, C. E., Schaller, G. E., Dangl, J. L., & Kieber, J. J. (2012). Two-Component Elements Mediate Interactions between Cytokinin and Salicylic Acid in Plant Immunity. *PLoS Genetics*, *8*(1), e1002448. https://doi.org/10.1371/journal.pgen.1002448

Ashikari, M., Sakakibara, H., Lin, S., Yamamoto, T., Takashi, T., Nishimura, A., Angeles, E. R., Qian, Q., Kitano, H., & Matsuoka, M. (2005). Cytokinin Oxidase Regulates Rice Grain Production. *Science*, *309*(5735), 741–745. https://doi.org/10.1126/science.1113373

Azizi, P., Rafii, M. Y., Maziah, M., Abdullah, S. N. A., Hanafi, M. M., Latif, M. A., Rashid, A. A., & Sahebi, M. (2015). Understanding the shoot apical meristem regulation: A study of the phytohormones, auxin and cytokinin, in rice. *Mechanisms of Development*, *135*, 1–15. https://doi.org/10.1016/j.mod.2014.11.001

Babosha, A. V. (2009). Regulation of resistance and susceptibility in wheat–powdery mildew pathosystem with exogenous cytokinins. *Journal of Plant Physiology*, *166*(17), 1892–1903. https://doi.org/10.1016/j.jplph.2009.05.014

Bartrina, I., Otto, E., Strnad, M., Werner, T., & Schmülling, T. (2011). Cytokinin Regulates the Activity of Reproductive Meristems, Flower Organ Size, Ovule Formation, and Thus Seed Yield in *Arabidopsis thaliana*. *The Plant Cell*, *23*(1), 69–80. https://doi.org/10.1105/tpc.110.079079

Bellin, D., Asai, S., Delledonne, M., & Yoshioka, H. (2013). Nitric Oxide as a Mediator for Defense Responses. *Molecular Plant-Microbe Interactions®*, *26*(3), 271–277. https://doi.org/10.1094/MPMI-09-12-0214-CR

Berardini, T. Z., Reiser, L., Li, D., Mezheritsky, Y., Muller, R., Strait, E., & Huala, E. (2015). The arabidopsis information resource: Making and mining the “gold standard” annotated reference plant genome: Tair: Making and Mining the “Gold Standard” Plant Genome. *Genesis*, *53*(8), 474–485. https://doi.org/10.1002/dvg.22877

Bergelson, J., & Purrington, C. B. (1996). Surveying Patterns in the Cost of Resistance in Plants. *The American Naturalist*, *148*(3), 536–558. https://doi.org/10.1086/285938

Berry, H. M., & Argueso, C. T. (2022). More than growth: Phytohormone-regulated transcription factors controlling plant immunity, plant development and plant architecture. *Current Opinion in Plant Biology*, *70*, 102309. https://doi.org/10.1016/j.pbi.2022.102309

Besnard, F., Rozier, F., & Vernoux, T. (2014). The AHP6 cytokinin signaling inhibitor mediates an auxin-cytokinin crosstalk that regulates the timing of organ initiation at the shoot apical meristem. *Plant Signaling & Behavior*, *9*(6), e28788. https://doi.org/10.4161/psb.28788

Bowling, S. A., Guo, A., Cao, H., Gordon, A. S., Klessig, D. F., & Dong, X. (1994). A mutation in Arabidopsis that leads to constitutive expression of systemic acquired resistance. *The Plant Cell*, *6*(12), 1845–1857. https://doi.org/10.1105/tpc.6.12.1845

Bowling, S. A., Clarke, J. D., Liu, Y., Klessig, D. F., & Dong, X. (1997). The cpr5 mutant of Arabidopsis expresses both NPR1-dependent and NPR1-independent resistance. *The plant cell*, *9*(9), 1573-1584. https://doi.org/10.1105/tpc.9.9.1573

Brown, J. K. M. (2002). Yield penalties of disease resistance in crops. *Current Opinion in Plant Biology*, *5*(4), 339–344. https://doi.org/10.1016/S1369-5266(02)00270-4

Canet, J. V., Dobón, A., Ibáñez, F., Perales, L., & Tornero, P. (2010). Resistance and biomass in Arabidopsis: A new model for Salicylic Acid perception. *Plant Biotechnology Journal*, *8*(2), 126–141. https://doi.org/10.1111/j.1467-7652.2009.00468.x

Chanclud, E., Kisiala, A., Emery, N. R. J., Chalvon, V., Ducasse, A., Romiti-Michel, C., Gravot, A., Kroj, T., & Morel, J.-B. (2016). Cytokinin Production by the Rice Blast Fungus Is a Pivotal Requirement for Full Virulence. *PLOS Pathogens*, *12*(2), e1005457. https://doi.org/10.1371/journal.ppat.1005457

Chen, S., Zhou, Y., Chen, Y., & Gu, J. (2018). fastp: An ultra-fast all-in-one FASTQ preprocessor. *Bioinformatics*, *34*(17), i884–i890. https://doi.org/10.1093/bioinformatics/bty560

Choi, J., Huh, S. U., Kojima, M., Sakakibara, H., Paek, K.-H., & Hwang, I. (2010). The Cytokinin-Activated Transcription Factor ARR2 Promotes Plant Immunity via TGA3/NPR1-Dependent Salicylic Acid Signaling in Arabidopsis. *Developmental Cell*, *19*(2), 284–295. https://doi.org/10.1016/j.devcel.2010.07.011

Clarke, J. D., Volko, S. M., Ledford, H., Ausubel, F. M., & Dong, X. (2000). Roles of Salicylic Acid, Jasmonic Acid, and Ethylene in *cpr* -Induced Resistance in Arabidopsis. *The Plant Cell*, *12*(11), 2175–2190. https://doi.org/10.1105/tpc.12.11.2175

Cohen, S. P., & Leach, J. E. (2020). High temperature-induced plant disease susceptibility: More than the sum of its parts. *Current Opinion in Plant Biology*, *56*, 235–241. https://doi.org/10.1016/j.pbi.2020.02.008

Coley, P. D., Bryant, J. P., & Chapin, F. S. (1985). Resource Availability and Plant Antiherbivore Defense. *Science*, *230*(4728), 895–899. https://doi.org/10.1126/science.230.4728.895

Daudi, A., & O'Brien, J. (2012). Detection of Hydrogen Peroxide by DAB Staining in Arabidopsis Leaves. *BIO-PROTOCOL*, *2*(18). https://doi.org/10.21769/BioProtoc.263

De Vleesschauwer, D., Gheysen, G., & Höfte, M. (2013). Hormone defense networking in rice: Tales from a different world. *Trends in Plant Science*, *18*(10), 555–565. https://doi.org/10.1016/j.tplants.2013.07.002

del Río, L. A. (2015). ROS and RNS in plant physiology: An overview. *Journal of Experimental Botany*, *66*(10), 2827–2837. https://doi.org/10.1093/jxb/erv099

Dodds, P. N., & Rathjen, J. P. (2010). Plant immunity: Towards an integrated view of plant–pathogen interactions. *Nature Reviews Genetics*, *11*(8), 539–548. https://doi.org/10.1038/nrg2812

Easterling, W., Aggarwal, P., Batima, P., Brander, K., Erda, L., Howden, M., ... & Tubiello, F. (2007). Climate Change 2007: Impacts, Adaptation, and Vulnerability. *Cambridge University Press. UK, Cambridge*, 273-313.

El-Kereamy, A., Bi, Y.-M., Mahmood, K., Ranathunge, K., Yaish, M. W., Nambara, E., & Rothstein, S. J. (2015). Overexpression of the CC-type glutaredoxin, OsGRX6 affects hormone and nitrogen status in rice plants. *Frontiers in Plant Science*, *6*. https://doi.org/10.3389/fpls.2015.00934

Galuszka, P., Popelková, H., Werner, T., Frébortová, J., Pospíšilová, H., Mik, V., Köllmer, I., Schmülling, T., & Frébort, I. (2007). Biochemical Characterization of Cytokinin Oxidases/Dehydrogenases from Arabidopsis thaliana Expressed in Nicotiana tabacum L. *Journal of Plant Growth Regulation*, *26*(3), 255–267. https://doi.org/10.1007/s00344-007-9008-5

Garg, R., Jhanwar, S., Tyagi, A. K., & Jain, M. (2010). Genome-wide survey and expression analysis suggest diverse roles of glutaredoxin gene family members during development and response to various stimuli in rice. *DNA research*, *17*(6), 353-367. https://doi.org/10.1093/dnares/dsq023

Gatz, C. (2013). From Pioneers to Team Players: TGA Transcription Factors Provide a Molecular Link Between Different Stress Pathways. *Molecular Plant-Microbe Interactions®*, *26*(2), 151–159. https://doi.org/10.1094/MPMI-04-12-0078-IA

Gómez-Gómez, L., Felix, G., & Boller, T. (1999). A single locus determines sensitivity to bacterial flagellin in Arabidopsis thaliana: Sensitivity of A. thaliana to bacterial flagellin. *The Plant Journal*, *18*(3), 277–284. https://doi.org/10.1046/j.1365-313X.1999.00451.x

González, R., Butković, A., Rivarez, M. P. S., & Elena, S. F. (2020). Natural variation in Arabidopsis thaliana rosette area unveils new genes involved in plant development. *Scientific Reports*, *10*(1), 17600. https://doi.org/10.1038/s41598-020-74723-4

Gordon, S. P., Chickarmane, V. S., Ohno, C., & Meyerowitz, E. M. (2009). Multiple feedback loops through cytokinin signaling control stem cell number within the *Arabidopsis* shoot meristem. *Proceedings of the National Academy of Sciences*, *106*(38), 16529–16534. https://doi.org/10.1073/pnas.0908122106

Gou, M., Shi, Z., Zhu, Y., Bao, Z., Wang, G., & Hua, J. (2012). The F-box protein CPR1/CPR30 negatively regulates R protein SNC1 accumulation: Negative regulation of SNC1 by CPR1/CPR30. *The Plant Journal*, *69*(3), 411–420. https://doi.org/10.1111/j.1365-313X.2011.04799.x

Guo, D. Y., Zhao, S. Y., Huang, L. L., Ma, C. Y., & Hao, L. (2014). Aluminum tolerance in Arabidopsis thaliana as affected by endogenous salicylic acid. *Biologia Plantarum*, *58*(4), 725–732. https://doi.org/10.1007/s10535-014-0439-0

Gupta, R., Pizarro, L., Leibman-Markus, M., Marash, I., & Bar, M. (2020). Cytokinin response induces immunity and fungal pathogen resistance, and modulates trafficking of the PRR LeEIX2 in tomato. *Molecular Plant Pathology*, *21*(10), 1287–1306. https://doi.org/10.1111/mpp.12978

Gutsche, N., Thurow, C., Zachgo, S., & Gatz, C. (2015). Plant-specific CC-type glutaredoxins: Functions in developmental processes and stress responses. *Biological Chemistry*, *396*(5), 495–509. https://doi.org/10.1515/hsz-2014-0300

Hao, L., Wang, Y., Xu, J., Feng, S.-D., Ma, C.-Y., Liu, C., Xu, X., Li, G.-Z., & Herbert, S. J. (2011). Role of endogenous salicylic acid in Arabidopsis response to elevated sulfur dioxide concentration. *Biologia Plantarum*, *55*(2), 297–304. https://doi.org/10.1007/s10535-011-0042-6

Hartmann, M., & Zeier, J. (2019). N-hydroxypipecolic acid and salicylic acid: A metabolic duo for systemic acquired resistance. *Current Opinion in Plant Biology*, *50*, 44–57. https://doi.org/10.1016/j.pbi.2019.02.006

Hirose, N., Takei, K., Kuroha, T., Kamada-Nobusada, T., Hayashi, H., & Sakakibara, H. (2007). Regulation of cytokinin biosynthesis, compartmentalization and translocation. *Journal of Experimental Botany*, *59*(1), 75–83. https://doi.org/10.1093/jxb/erm157

Hong, J. K., Yun, B.-W., Kang, J.-G., Raja, M. U., Kwon, E., Sorhagen, K., Chu, C., Wang, Y., & Loake, G. J. (2008). Nitric oxide function and signalling in plant disease resistance. *Journal of Experimental Botany*, *59*(2), 147–154. https://doi.org/10.1093/jxb/erm244

Huot, B., Yao, J., Montgomery, B. L., & He, S. Y. (2014). Growth–Defense Tradeoffs in Plants: A Balancing Act to Optimize Fitness. *Molecular Plant*, *7*(8), 1267–1287. https://doi.org/10.1093/mp/ssu049

Ishida, K., Yamashino, T., Yokoyama, A., & Mizuno, T. (2008). Three Type-B Response Regulators, ARR1, ARR10 and ARR12, Play Essential but Redundant Roles in Cytokinin Signal Transduction Throughout the Life Cycle of Arabidopsis thaliana. *Plant and Cell Physiology*, *49*(1), 47–57. https://doi.org/10.1093/pcp/pcm165

Jiang, C.-J., Shimono, M., Sugano, S., Kojima, M., Liu, X., Inoue, H., Sakakibara, H., & Takatsuji, H. (2013). Cytokinins Act Synergistically with Salicylic Acid to Activate Defense Gene Expression in Rice. *Molecular Plant-Microbe Interactions®*, *26*(3), 287–296. https://doi.org/10.1094/MPMI-06-12-0152-R

Jung, J.-Y., Ahn, J. H., & Schachtman, D. P. (2018). CC-type glutaredoxins mediate plant response and signaling under nitrate starvation in Arabidopsis. *BMC Plant Biology*, *18*(1), 281. https://doi.org/10.1186/s12870-018-1512-1

Kerwin, R., Feusier, J., Corwin, J., Rubin, M., Lin, C., Muok, A., Larson, B., Li, B., Joseph, B., Francisco, M., Copeland, D., Weinig, C., & Kliebenstein, D. J. (2015). Natural genetic variation in Arabidopsis thaliana defense metabolism genes modulates field fitness. *ELife*, *4*, e05604. https://doi.org/10.7554/eLife.05604

Kesarwani, M., Yoo, J., & Dong, X. (2007). Genetic Interactions of TGA Transcription Factors in the Regulation of Pathogenesis-Related Genes and Disease Resistance in Arabidopsis. *Plant Physiology*, *144*(1), 336–346. https://doi.org/10.1104/pp.106.095299

Khan, M., Ali, S., Al Azzawi, T. N. I., Saqib, S., Ullah, F., Ayaz, A., & Zaman, W. (2023). The Key Roles of ROS and RNS as a Signaling Molecule in Plant–Microbe Interactions. *Antioxidants*, *12*(2), 268. https://doi.org/10.3390/antiox12020268

Kieber, J. J., & Schaller, G. E. (2014). Cytokinins. *The Arabidopsis Book*, *12*, e0168. https://doi.org/10.1199/tab.0168

Kim, D., Paggi, J. M., Park, C., Bennett, C., & Salzberg, S. L. (2019). Graph-based genome alignment and genotyping with HISAT2 and HISAT-genotype. *Nature Biotechnology*, *37*(8), 907–915. https://doi.org/10.1038/s41587-019-0201-4

Kliebenstein, D. J. (2016). False idolatry of the mythical growth versus immunity tradeoff in molecular systems plant pathology. *Physiological and Molecular Plant Pathology*, *95*, 55–59. https://doi.org/10.1016/j.pmpp.2016.02.004

Kojima, M., Kamada-Nobusada, T., Komatsu, H., Takei, K., Kuroha, T., Mizutani, M., ... & Sakakibara, H. (2009). Highly sensitive and high-throughput analysis of plant hormones using MS-probe modification and liquid chromatography–tandem mass spectrometry: an application for hormone profiling in Oryza sativa. *Plant and Cell Physiology*, *50*(7), 1201-1214. https://doi.org/10.1093/pcp/pcp057

Kudo, T., Kiba, T., & Sakakibara, H. (2010). Metabolism and Long-distance Translocation of Cytokinins. *Journal of Integrative Plant Biology*, *52*(1), 53–60. https://doi.org/10.1111/j.1744-7909.2010.00898.x

Lai, Z., Schluttenhofer, C. M., Bhide, K., Shreve, J., Thimmapuram, J., Lee, S. Y., Yun, D.-J., & Mengiste, T. (2014). MED18 interaction with distinct transcription factors regulates multiple plant functions. *Nature Communications*, *5*(1), 3064. https://doi.org/10.1038/ncomms4064

Landrein, B., Formosa-Jordan, P., Malivert, A., Schuster, C., Melnyk, C. W., Yang, W., Turnbull, C., Meyerowitz, E. M., Locke, J. C. W., & Jönsson, H. (2018). Nitrate modulates stem cell dynamics in *Arabidopsis* shoot meristems through cytokinins. *Proceedings of the National Academy of Sciences*, *115*(6), 1382–1387. https://doi.org/10.1073/pnas.1718670115

Laporte, D., Olate, E., Salinas, P., Salazar, M., Jordana, X., & Holuigue, L. (2012). Glutaredoxin GRXS13 plays a key role in protection against photooxidative stress in Arabidopsis. *Journal of Experimental Botany*, *63*(1), 503–515. https://doi.org/10.1093/jxb/err301

Lefevere, H., Bauters, L., & Gheysen, G. (2020). Salicylic Acid Biosynthesis in Plants. *Frontiers in Plant Science*, *11*, 338. https://doi.org/10.3389/fpls.2020.00338

Leibfried, A., To, J. P. C., Busch, W., Stehling, S., Kehle, A., Demar, M., Kieber, J. J., & Lohmann, J. U. (2005). WUSCHEL controls meristem function by direct regulation of cytokinin-inducible response regulators. *Nature*, *438*(7071), 1172–1175. https://doi.org/10.1038/nature04270

Li, N., Muthreich, M., Huang, L., Thurow, C., Sun, T., Zhang, Y., & Gatz, C. (2019a). TGACG-BINDING FACTORs (TGAs) and TGA-interacting CC-type glutaredoxins modulate hyponastic growth in *Arabidopsis thaliana*. *New Phytologist*, *221*(4), 1906–1918. https://doi.org/10.1111/nph.15496

Li, S., Lauri, A., Ziemann, M., Busch, A., Bhave, M., & Zachgo, S. (2009). Nuclear Activity of ROXY1, a Glutaredoxin Interacting with TGA Factors, Is Required for Petal Development in *Arabidopsis thaliana*. *The Plant Cell*, *21*(2), 429–441. https://doi.org/10.1105/tpc.108.064477

Li, X., Clarke, J. D., Zhang, Y., & Dong, X. (2001). Activation of an EDS1-Mediated *R* -Gene Pathway in the *snc1* Mutant Leads to Constitutive, NPR1-Independent Pathogen Resistance. *Molecular Plant-Microbe Interactions®*, *14*(10), 1131–1139. https://doi.org/10.1094/MPMI.2001.14.10.1131

Li, Y., Yang, Y., Hu, Y., Liu, H., He, M., Yang, Z., Kong, F., Liu, X., & Hou, X. (2019b). DELLA and EDS1 Form a Feedback Regulatory Module to Fine-Tune Plant Growth–Defense Tradeoff in Arabidopsis. *Molecular Plant*, *12*(11), 1485–1498. https://doi.org/10.1016/j.molp.2019.07.006

Liao, Y., Smyth, G. K., & Shi, W. (2014). featureCounts: An efficient general purpose program for assigning sequence reads to genomic features. *Bioinformatics*, *30*(7), 923–930. https://doi.org/10.1093/bioinformatics/btt656

Lillo, C., Meyer, C., Lea, U. S., Provan, F., & Oltedal, S. (2004). Mechanism and importance of post-translational regulation of nitrate reductase. *Journal of Experimental Botany*, *55*(401), 1275–1282. https://doi.org/10.1093/jxb/erh132

Lindermayr, C., & Durner, J. (2009). S-Nitrosylation in plants: Pattern and function. *Journal of Proteomics*, *73*(1), 1–9. https://doi.org/10.1016/j.jprot.2009.07.002

Lindermayr, C., Sell, S., Müller, B., Leister, D., & Durner, J. (2010). Redox Regulation of the NPR1-TGA1 System of *Arabidopsis thaliana* by Nitric Oxide. *The Plant Cell*, *22*(8), 2894–2907. https://doi.org/10.1105/tpc.109.066464

Liu, W.-Z., Kong, D.-D., Gu, X.-X., Gao, H.-B., Wang, J.-Z., Xia, M., Gao, Q., Tian, L.-L., Xu, Z.-H., Bao, F., Hu, Y., Ye, N.-S., Pei, Z.-M., & He, Y.-K. (2013). Cytokinins can act as suppressors of nitric oxide in *Arabidopsis*. *Proceedings of the National Academy of Sciences*, *110*(4), 1548–1553. https://doi.org/10.1073/pnas.1213235110

Love, M. I., Huber, W., & Anders, S. (2014). Moderated estimation of fold change and dispersion for RNA-seq data with DESeq2. *Genome Biology*, *15*(12), 550. https://doi.org/10.1186/s13059-014-0550-8

McIntyre, K. E., Bush, D. R., & Argueso, C. T. (2021). Cytokinin Regulation of Source-Sink Relationships in Plant-Pathogen Interactions. *Frontiers in Plant Science*, *12*, 677585. https://doi.org/10.3389/fpls.2021.677585

Miller, C. O., Skoog, F., Okumura, F. S., Von Saltza, M. H., & Strong, F. M. (1956). Isolation, Structure and Synthesis of Kinetin, a Substance Promoting Cell Division [1,2]. *Journal of the American Chemical Society*, *78*(7), 1375–1380. https://doi.org/10.1021/ja01588a032

Miyawaki, K., Matsumoto-Kitano, M., & Kakimoto, T. (2004). Expression of cytokinin biosynthetic isopentenyltransferase genes in *Arabidopsis*: Tissue specificity and regulation

by auxin, cytokinin, and nitrate. *The Plant Journal*, *37*(1), 128–138. https://doi.org/10.1046/j.1365-313X.2003.01945.x

Miyawaki, K., Tarkowski, P., Matsumoto-Kitano, M., Kato, T., Sato, S., Tarkowska, D., Tabata, S., Sandberg, G., & Kakimoto, T. (2006). Roles of *Arabidopsis* ATP/ADP isopentenyltransferases and tRNA isopentenyltransferases in cytokinin biosynthesis. *Proceedings of the National Academy of Sciences*, *103*(44), 16598–16603. https://doi.org/10.1073/pnas.0603522103

Monson, R. K., Trowbridge, A. M., Lindroth, R. L., & Lerdau, M. T. (2022). Coordinated resource allocation to plant growth–defense tradeoffs. *New Phytologist*, *233*(3), 1051–1066. https://doi.org/10.1111/nph.17773

Mur, L. A. J., Prats, E., Pierre, S., Hall, M. A., & Hebelstrup, K. H. (2013). Integrating nitric oxide into salicylic acid and jasmonic acid/ ethylene plant defense pathways. *Frontiers in Plant Science*, *4*. https://doi.org/10.3389/fpls.2013.00215

Ndamukong, I., Abdallat, A. A., Thurow, C., Fode, B., Zander, M., Weigel, R., & Gatz, C. (2007). SA-inducible Arabidopsis glutaredoxin interacts with TGA factors and suppresses JA-responsive PDF1.2 transcription: Interaction of glutaredoxin with TGA factors. *The Plant Journal*, *50*(1), 128–139. https://doi.org/10.1111/j.1365-313X.2007.03039.x

Ning, Y., Liu, W., & Wang, G.-L. (2017). Balancing Immunity and Yield in Crop Plants. *Trends in Plant Science*, *22*(12), 1069–1079. https://doi.org/10.1016/j.tplants.2017.09.010

Olas, J. J., Van Dingenen, J., Abel, C., Działo, M. A., Feil, R., Krapp, A., Schlereth, A., & Wahl, V. (2019). Nitrate acts at the *Arabidopsis thaliana* shoot apical meristem to regulate flowering time. *New Phytologist*, *223*(2), 814–827. https://doi.org/10.1111/nph.15812

Pasternak, T., Groot, E. P., Kazantsev, F. V., Teale, W., Omelyanchuk, N., Kovrizhnykh, V., Palme, K., & Mironova, V. V. (2019). Salicylic Acid Affects Root Meristem Patterning via Auxin Distribution in a Concentration-Dependent Manner. *Plant Physiology*, *180*(3), 1725–1739. https://doi.org/10.1104/pp.19.00130

Perales, M., & Reddy, G. V. (2012). Stem cell maintenance in shoot apical meristems. *Current opinion in plant biology*, *15*(1), 10-16. https://doi.org/10.1016/j.pbi.2011.10.008

Pieterse, C. M. J., Van der Does, D., Zamioudis, C., Leon-Reyes, A., & Van Wees, S. C. M. (2012). Hormonal Modulation of Plant Immunity. *Annual Review of Cell and Developmental Biology*, *28*(1), 489–521. https://doi.org/10.1146/annurev-cellbio-092910-154055

Rao, M. V., Paliyath, G., Ormrod, D. P., Murr, D. P., & Watkins, C. B. (1997). Influence of Salicylic Acid on H2O2 Production, Oxidative Stress, and H2O2-Metabolizing Enzymes (Salicylic Acid-Mediated Oxidative Damage Requires H2O2). *Plant Physiology*, *115*(1), 137–149. https://doi.org/10.1104/pp.115.1.137

Ray, D. K., Mueller, N. D., West, P. C., & Foley, J. A. (2013). Yield Trends Are Insufficient to Double Global Crop Production by 2050. *PLoS ONE*, *8*(6), e66428. https://doi.org/10.1371/journal.pone.0066428

Ray, D. K., Ramankutty, N., Mueller, N. D., West, P. C., & Foley, J. A. (2012). Recent patterns of crop yield growth and stagnation. *Nature Communications*, *3*(1), 1293. https://doi.org/10.1038/ncomms2296

Rhoades, D.F. (1979). Evolution of plant chemical defense against herbivores. Herbivores: Their Interaction with Secondary Plant Metabolites (eds G.A. Rosenthal & D.H. Janzen), 4–55. Academic Press, Orlando, FL.

Rijpkema, A. S., Vandenbussche, M., Koes, R., Heijmans, K., & Gerats, T. (2010). Variations on a theme: Changes in the floral ABCs in angiosperms. *Seminars in Cell & Developmental Biology*, *21*(1), 100–107. https://doi.org/10.1016/j.semcdb.2009.11.002

Romanov, G. A., Lomin, S. N., Rakova, N. Yu., Heyl, A., & Schmülling, T. (2008). Does NO play a role in cytokinin signal transduction? *FEBS Letters*, *582*(6), 874–880. https://doi.org/10.1016/j.febslet.2008.02.016

Rouhier, N., Gelhaye, E., & Jacquot, J.-P. (2004). Plant glutaredoxins: Still mysterious reducing systems. *Cellular and Molecular Life Sciences CMLS*, *61*(11), 1266–1277. https://doi.org/10.1007/s00018-004-3410-y

Rouhier, N., Lemaire, S. D., & Jacquot, J.-P. (2008). The Role of Glutathione in Photosynthetic Organisms: Emerging Functions for Glutaredoxins and Glutathionylation. *Annual Review of Plant Biology*, *59*(1), 143–166. https://doi.org/10.1146/annurev.arplant.59.032607.092811

Running, M. P., & Meyerowitz, E. M. (1996). Mutations in the PERIANTHIA gene of Arabidopsis specifically alter floral organ number and initiation pattern. *Development*, *122*(4), 1261–1269. https://doi.org/10.1242/dev.122.4.1261

Rustérucci, C., Espunya, M. C., Díaz, M., Chabannes, M., & Martínez, M. C. (2007). *S* -Nitrosoglutathione Reductase Affords Protection against Pathogens in Arabidopsis, Both Locally and Systemically. *Plant Physiology*, *143*(3), 1282–1292. https://doi.org/10.1104/pp.106.091686

Sachdev, S., Ansari, S. A., Ansari, M. I., Fujita, M., & Hasanuzzaman, M. (2021). Abiotic Stress and Reactive Oxygen Species: Generation, Signaling, and Defense Mechanisms. *Antioxidants*, *10*(2), 277. https://doi.org/10.3390/antiox10020277

Sakakibara, H. (2006). CYTOKININS: Activity, Biosynthesis, and Translocation. *Annual Review of Plant Biology*, *57*(1), 431–449. https://doi.org/10.1146/annurev.arplant.57.032905.105231

Sakakibara, H. (2021). Cytokinin biosynthesis and transport for systemic nitrogen signaling. *The Plant Journal*, *105*(2), 421–430. https://doi.org/10.1111/tpj.15011

Sakamoto, T., Sakakibara, H., Kojima, M., Yamamoto, Y., Nagasaki, H., Inukai, Y., Sato, Y., & Matsuoka, M. (2006). Ectopic Expression of KNOTTED1-Like Homeobox Protein Induces Expression of Cytokinin Biosynthesis Genes in Rice. *Plant Physiology*, *142*(1), 54–62. https://doi.org/10.1104/pp.106.085811

Saleh, A., Withers, J., Mohan, R., Marqués, J., Gu, Y., Yan, S., Zavaliev, R., Nomoto, M., Tada, Y., & Dong, X. (2015). Posttranslational Modifications of the Master Transcriptional Regulator NPR1 Enable Dynamic but Tight Control of Plant Immune Responses. *Cell Host & Microbe*, *18*(2), 169–182. https://doi.org/10.1016/j.chom.2015.07.005

Schwarz, I., Scheirlinck, M.-T., Otto, E., Bartrina, I., Schmidt, R.-C., & Schmülling, T. (2020). Cytokinin regulates the activity of the inflorescence meristem and components of seed yield in oilseed rape. *Journal of Experimental Botany*, *71*(22), 7146–7159. https://doi.org/10.1093/jxb/eraa419

Seligman, K., Saviani, E. E., Oliveira, H. C., Pinto-Maglio, C. A. F., & Salgado, I. (2008). Floral Transition and Nitric Oxide Emission During Flower Development in Arabidopsis thaliana is Affected in Nitrate Reductase-Deficient Plants. *Plant and Cell Physiology*, *49*(7), 1112–1121. https://doi.org/10.1093/pcp/pcn089

Shen, Q., Wang, Y.-T., Tian, H., & Guo, F.-Q. (2013). Nitric Oxide Mediates Cytokinin Functions in Cell Proliferation and Meristem Maintenance in Arabidopsis. *Molecular Plant*, *6*(4), 1214–1225. https://doi.org/10.1093/mp/sss148

Smyth, D. R., Bowman, J. L., & Meyerowitz, E. M. (1990). Early flower development in Arabidopsis. *The Plant Cell*, *2*(8), 755–767. https://doi.org/10.1105/tpc.2.8.755

Spoel, S. H., Johnson, J. S., & Dong, X. (2007). Regulation of tradeoffs between plant defenses against pathogens with different lifestyles. *Proceedings of the National Academy of Sciences*, *104*(47), 18842–18847. https://doi.org/10.1073/pnas.0708139104

Strange, R. N., & Scott, P. R. (2005). Plant Disease: A Threat to Global Food Security. *Annual Review of Phytopathology*, *43*(1), 83–116. https://doi.org/10.1146/annurev.phyto.43.113004.133839

Su, Y.-H., Liu, Y.-B., & Zhang, X.-S. (2011). Auxin–Cytokinin Interaction Regulates Meristem Development. *Molecular Plant*, *4*(4), 616–625. https://doi.org/10.1093/mp/ssr007

Tada, Y., Spoel, S. H., Pajerowska-Mukhtar, K., Mou, Z., Song, J., Wang, C., Zuo, J., & Dong, X. (2008). Plant Immunity Requires Conformational Charges of NPR1 via S-Nitrosylation and Thioredoxins. *Science*, *321*(5891), 952–956. https://doi.org/10.1126/science.1156970

Takei, K., Ueda, N., Aoki, K., Kuromori, T., Hirayama, T., Shinozaki, K., Yamaya, T., & Sakakibara, H. (2004). AtIPT3 is a Key Determinant of Nitrate-Dependent Cytokinin Biosynthesis in Arabidopsis. *Plant and Cell Physiology*, *45*(8), 1053–1062. https://doi.org/10.1093/pcp/pch119

Taleski, M., Chapman, K., Novák, O., Schmülling, T., Frank, M., & Djordjevic, M. A. (2022). *CEP peptide and cytokinin pathways converge on CEPD glutaredoxins to inhibit root growth* [Preprint]. Plant Biology. https://doi.org/10.1101/2022.07.05.498042

Taleski, M., Imin, N., & Djordjevic, M. A. (2018). CEP peptide hormones: Key players in orchestrating nitrogen-demand signalling, root nodulation, and lateral root development. *Journal of Experimental Botany*, *69*(8), 1829–1836. https://doi.org/10.1093/jxb/ery037

Thomas, P. D., Ebert, D., Muruganujan, A., Mushayahama, T., Albou, L., & Mi, H. (2022). PANTHER: Making genome-scale phylogenetics accessible to all. *Protein Science*, *31*(1), 8–22. https://doi.org/10.1002/pro.4218

Tian, D., Traw, M. B., Chen, J. Q., Kreitman, M., & Bergelson, J. (2003). Fitness costs of R-gene-mediated resistance in Arabidopsis thaliana. *Nature*, *423*(6935), 74–77. https://doi.org/10.1038/nature01588

Tiwari, M., Sharma, D., Singh, M., Tripathi, R. D., & Trivedi, P. K. (2014). Expression of OsMATE1 and OsMATE2 alters development, stress responses and pathogen susceptibility in Arabidopsis. *Scientific Reports*, *4*(1), 3964. https://doi.org/10.1038/srep03964

Tornero, P., & Dangl, J. L. (2002). A high-throughput method for quantifying growth of phytopathogenic bacteria in Arabidopsis thaliana: Counting bacteria in Arabidopsis. *The Plant Journal*, *28*(4), 475–481. https://doi.org/10.1046/j.1365-313X.2001.01136.x

Toufighi, K., Brady, S. M., Austin, R., Ly, E., & Provart, N. J. (2005). The Botany Array Resource: E-Northerns, Expression Angling, and promoter analyses: The Botany Array Resource. *The Plant Journal*, *43*(1), 153–163. https://doi.org/10.1111/j.1365-313X.2005.02437.x

Tsago, Y., Chen, Z., Cao, H., Sunusi, M., Khan, A. U., Shi, C., & Jin, X. (2020). Rice gene, OsCKX2-2, regulates inflorescence and grain size by increasing endogenous cytokinin content. *Plant Growth Regulation*, *92*(2), 283–294. https://doi.org/10.1007/s10725-020-00637-w

van Wersch, R., Li, X., & Zhang, Y. (2016). Mighty Dwarfs: Arabidopsis Autoimmune Mutants and Their Usages in Genetic Dissection of Plant Immunity. *Frontiers in Plant Science*, *7*. https://doi.org/10.3389/fpls.2016.01717

Wang, H., Lu, Y., Liu, P., Wen, W., Zhang, J., Ge, X., & Xia, Y. (2013). The ammonium/nitrate ratio is an input signal in the temperature-modulated, *SNC1* -mediated and *EDS1* -dependent autoimmunity of *nudt6-2 nudt7*. *The Plant Journal*, *73*(2), 262–275. https://doi.org/10.1111/tpj.12032

Wang, Y.-Y., Wang, Y., Li, G.-Z., & Hao, L. (2019). Salicylic acid-altering Arabidopsis plant response to cadmium exposure: Underlying mechanisms affecting antioxidation and photosynthesis-related processes. *Ecotoxicology and Environmental Safety*, *169*, 645–653. https://doi.org/10.1016/j.ecoenv.2018.11.062

Wasternack, C. (2017). A plant's balance of growth and defense – revisited. *New Phytologist*, *215*(4), 1291–1294. https://doi.org/10.1111/nph.14720

Werner, T., Motyka, V., Laucou, V., Smets, R., Van Onckelen, H., & Schmülling, T. (2003). Cytokinin-Deficient Transgenic Arabidopsis Plants Show Multiple Developmental Alterations Indicating Opposite Functions of Cytokinins in the Regulation of Shoot and Root Meristem Activity. *The Plant Cell*, *15*(11), 2532–2550. https://doi.org/10.1105/tpc.014928

Winter, C. M., Austin, R. S., Blanvillain-Baufumé, S., Reback, M. A., Monniaux, M., Wu, M.-F., Sang, Y., Yamaguchi, A., Yamaguchi, N., Parker, J. E., Parcy, F., Jensen, S. T., Li, H., & Wagner, D. (2011). LEAFY Target Genes Reveal Floral Regulatory Logic, cis Motifs, and a Link to Biotic Stimulus Response. *Developmental Cell*, *20*(4), 430–443. https://doi.org/10.1016/j.devcel.2011.03.019

Wu, J., Zhu, W., & Zhao, Q. (2023). Salicylic acid biosynthesis is not from phenylalanine in *Arabidopsis*. *Journal of Integrative Plant Biology*, jipb.13410. https://doi.org/10.1111/jipb.13410

Xiao, S., Hu, Q., Zhang, X., Si, H., Liu, S., Chen, L., Chen, K., Berne, S., Yuan, D., Lindsey, K., Zhang, X., & Zhu, L. (2021). Orchestration of plant development and defense by indirect crosstalk of salicylic acid and brassinosteorid signaling via transcription factor GhTINY2. *Journal of Experimental Botany*, *72*(13), 4721–4743. https://doi.org/10.1093/jxb/erab186

Xing, S., & Zachgo, S. (2008). ROXY1 and ROXY2, two Arabidopsis glutaredoxin genes, are required for anther development. *The Plant Journal*, *53*(5), 790–801. https://doi.org/10.1111/j.1365-313X.2007.03375.x

Yan, J., Zhang, C., Gu, M., Bai, Z., Zhang, W., Qi, T., Cheng, Z., Peng, W., Luo, H., Nan, F., Wang, Z., & Xie, D. (2009). The *Arabidopsis* CORONATINE INSENSITIVE1 Protein Is a Jasmonate Receptor. *The Plant Cell*, *21*(8), 2220–2236. https://doi.org/10.1105/tpc.109.065730

Yang, D.-L., Yang, Y., & He, Z. (2013). Roles of Plant Hormones and Their Interplay in Rice Immunity. *Molecular Plant*, *6*(3), 675–685. https://doi.org/10.1093/mp/sst056

Yang, R. S., Xu, F., Wang, Y. M., Zhong, W. S., Dong, L., Shi, Y. N., Tang, T. J., Sheng, H. J., Jackson, D., & Yang, F. (2021a). Glutaredoxins regulate maize inflorescence meristem development via redox control of TGA transcriptional activity. *Nature Plants*, *7*(12), 1589–1601. https://doi.org/10.1038/s41477-021-01029-2

Yang, W., Cortijo, S., Korsbo, N., Roszak, P., Schiessl, K., Gurzadyan, A., Wightman, R., Jönsson, H., & Meyerowitz, E. (2021b). Molecular mechanism of cytokinin-activated cell division in *Arabidopsis*. *Science*, *371*(6536), 1350–1355. https://doi.org/10.1126/science.abe2305

Zander, M., Chen, S., Imkampe, J., Thurow, C., & Gatz, C. (2012). Repression of the Arabidopsis thaliana Jasmonic Acid/Ethylene-Induced Defense Pathway by TGA-Interacting Glutaredoxins Depends on Their C-Terminal ALWL Motif. *Molecular Plant*, *5*(4), 831–840. https://doi.org/10.1093/mp/ssr113

Zangerl, A. R., & Bazzaz, F. A. (1992). Theory and pattern in plant defense allocation. Plant Resistance to Herbivores and Pathogens (eds S. Fritz & E. L. Simms), 363–391. The University of Chicago Press, Chicago.

Zeng, J., Dong, Z., Wu, H., Tian, Z., & Zhao, Z. (2017). Redox regulation of plant stem cell fate. *The EMBO Journal*, *36*(19), 2844–2855. https://doi.org/10.15252/embj.201695955

Zhang, Y., Goritschnig, S., Dong, X., & Li, X. (2003). A Gain-of-Function Mutation in a Plant Disease Resistance Gene Leads to Constitutive Activation of Downstream Signal Transduction Pathways in *suppressor of npr1-1* , *constitutive 1*. *The Plant Cell*, *15*(11), 2636–2646. https://doi.org/10.1105/tpc.015842

Zhao, Z., Andersen, S. U., Ljung, K., Dolezal, K., Miotk, A., Schultheiss, S. J., & Lohmann, J. U. (2010). Hormonal control of the shoot stem-cell niche. *Nature*, *465*(7301), 1089–1092. https://doi.org/10.1038/nature09126

Zhou, D., Shen, W., Cui, Y., Liu, Y., Zheng, X., Li, Y., Wu, M., Fang, S., Liu, C., Tang, M., Yi, Y., Zhao, M., & Chen, L. (2021). APICAL SPIKELET ABORTION (ASA) Controls Apical Panicle Development in Rice by Regulating Salicylic Acid Biosynthesis. *Frontiers in Plant Science*, *12*, 636877. https://doi.org/10.3389/fpls.2021.636877

Zhu, Y., Du, B., Qian, J., Zou, B., & Hua, J. (2013). Disease Resistance Gene-Induced Growth Inhibition Is Enhanced by *rcd1* Independent of Defense Activation in Arabidopsis. *Plant Physiology*, *161*(4), 2005–2013. https://doi.org/10.1104/pp.112.213363

Zhu, Y., Qian, W., & Hua, J. (2010). Temperature Modulates Plant Defense Responses through NB-LRR Proteins. *PLoS Pathogens*, *6*(4), e1000844. https://doi.org/10.1371/journal.ppat.1000844

Zottini, M., Costa, A., De Michele, R., Ruzzene, M., Carimi, F., & Lo Schiavo, F. (2007). Salicylic acid activates nitric oxide synthesis in Arabidopsis. *Journal of Experimental Botany*, *58*(6), 1397–1405. https://doi.org/10.1093/jxb/erm001

Zubo, Y. O., Blakley, I. C., Yamburenko, M. V., Worthen, J. M., Street, I. H., Franco-Zorrilla, J. M., Zhang, W., Hill, K., Raines, T., Solano, R., Kieber, J. J., Loraine, A. E., & Schaller, G. E. (2017). Cytokinin induces genome-wide binding of the type-B response regulator ARR10 to regulate growth and development in *Arabidopsis*. *Proceedings of the National Academy of Sciences*, *114*(29). https://doi.org/10.1073/pnas.1620749114

Zürcher, E., Tavor-Deslex, D., Lituiev, D., Enkerli, K., Tarr, P. T., & Müller, B. (2013). A Robust and Sensitive Synthetic Sensor to Monitor the Transcriptional Output of the Cytokinin Signaling Network in Planta. *Plant Physiology*, *161*(3), 1066–1075. https://doi.org/10.1104/pp.112.211763

APPENDIX: CK-SA CROSSTALK ANALYSIS AMONG DIVERSE ARABIDOPSIS ACCESSIONS

Introduction

Models are derivative tools to analyze relationships and connectivity of nodes within a specific network, that have yet been able to capture all the complexity of biological systems. But with a knowledgeable understanding of the limitations, computational and mathematical modeling can yield insightful associations and predictive outcomes. Particularly useful in integration of large datasets, the merging of modeling techniques and biological data has been achieved in plant systems using different approaches with varying degrees of complexity (Yuan et al., 2008; Prusinkiewicz & Runions, 2012; Sheth & Tacker, 2014; Matthews & Marshall-Colón, 2021; Soualiou et al., 2021). Of particular interest, phytohormone networks have successfully been modeled (Middleton et al., 2012; Liu, Rowe, & Lindsey, 2014; Altmann et al., 2020; Clark et al., 2021; Cammarata et al., 2022), though a standalone CK-SA crosstalk model has yet to be accomplished.

Natural variation refers to genetic differences between populations of the same species. As plants have adapted to their local environment, populations acquire random mutations resulting in phenotype divergence but not to the point of speciation. These variants or accessions can then be used to identify genetic markers associated with specific phenotypic traits. As a model organism historically used to study genetic architecture, Arabidopsis is a useful candidate for plant evolution and genetic diversity observations with upwards of 700 accessions collected (Berardini et al., 2015). A genome-wide association (GWA) study is a method of correlating mutations to phenotypic traits. In turn, phenotypic differences can be linked to genetic perturbations at specific loci, implicating individual genes as responsible for a given trait. Although GWA studies were first used in humans (Hirschhorn & Daly, 2005), these types of studies have been successful in Arabidopsis. For example, the GWA method was

applied to examine phytohormone crosstalk in Proietti et al., 2018. The authors found numerous loci associated with mediating SA-JA crosstalk by using gene expression data of a JA marker gene after hormone treatment for their GWA study. The genes corresponding with the loci found were confirmed to influence SA-JA crosstalk when mutated (Proietti et al., 2018).

Here, we show a detailed analysis of the dynamics of SA and CK crosstalk, as determined by gene expression as a proxy for signaling levels. Determination of hormone signaling dynamics is an essential part of any future efforts for model construction. Additionally, we test whether the CK-SA crosstalk is modified in response to natural variation resulting from adaptions to the environment. Future efforts in this project include testing a model constructed with the Col-0 accession against other Arabidopsis accessions and GWA mapping to identify novel loci mediating CK-SA crosstalk. We hope this research will lend to candidate genes that act as central control hubs of hormone crosstalk.

Methods & Results

To evaluate the transcriptional regulation CK and SA application have on both pathways, two marker genes associated with each hormonal pathway were chosen for gene expression analyses by qRT-PCR. Type-A *ARR7* and *CRF6* were chosen to monitor CK-regulated responses, while *NIM1-INTERACTING 1* (*NIMIN1*) and *PR1* were used as SA-regulated markers. Both *ARR7* and *NIMIN1* are early response, negative regulators of their respective pathways. *CRF6* and *PR1* are induced later in response to CK and SA, respectively. Utilizing genes with different response times (early and late genes) allowed us to determine differences in signaling responses after hormone induction and perception within a 24 h timecourse.

Two-week-old Col-0 wildtype seedlings grown on MS plates were transferred to liquid MS. One hour later the media was spiked with 100 μM 6-benzylaminopurine (BA), a synthetic cytokinin, or 100 μM SA. Whole seedling tissue was harvested at 0.25, 1, 6, 9, 12, and 24 h

after hormone treatment. RNA was extracted, subjected to quality control, and cDNA made, followed by analysis of gene expression by qRT-PCR.

The results of these experiments showed that after treatment with CK, *ARR7* transcription is promptly induced (Figure 15A), which correlates with kinetic studies showing *ARR7* expression peaks at 40 minutes after exogenous CK application (D'agostino et al., 2000). It was previously found that *CRF6* is steadily upregulated until 8 h after CK treatment (Rashotte et al., 2006). Similarly, in our data, *CRF6* exhibits a gradual increase in expression (Figure 15A). Both genes appear to plateau between 12 and 24 h. On the other hand, CK induces the negative SA-regulator, *NIMIN1*, and inhibits *PR1* expression (Figure 15B), suggesting an inhibitory effect of CK on SA signaling. Both *ARR7* and *CRF6* were down regulated in the presence of SA at each timepoint after 0.25 h (Figure 15C), which directly corresponds to our earlier findings in Figure 1. As expected, *NIMIN1* and *PR1* are upregulated by SA treatment, both plateauing between 12 and 24 h (Figure 15D). Although earlier work showed a gradual increase in expression of *NMIN1* after SA treatment (Blanco et al., 2009), we observed a very strong induction even at 0.25 h. As in Ward et al., 1991, maximal *PR1* expression happens at later timepoints. CK and SA treatment both transiently induced gene expression of the opposite pathway at 0.25 h (Figure 15B and 15C). This could indicate large, rapid transcriptional shifts occurring in response to stimuli, as the plant attempts to adapt to the new environment.

We acquired a set of 96 Arabidopsis accessions from the Arabidopsis Biological Resource Center (ABRC; https://abrc.osu.edu/) (CS22660). To analyze the robustness of the CK-SA crosstalk modeled in the Col-0 background, we performed liquid hormone inductions (as described for Figure 15 above) on a subset of these accessions (Table 4). qRT-PCR was performed as previously described, using only one marker gene per hormone and a single 3 h timepoint. After CK induction, all accessions have induced *ARR7* expression by 3 h, yet greater variation in *PR1* response is observed (Figure 16). While Col-0 inhibited expression in our timecourse experiments, the An-1 accession showed induced transcription of *PR1* in response

to CK. Likewise, deviation in expression in response to SA treatment is also observed. With the exception of Ws-2, *PR1* is upregulated by SA at 3 h in all other accessions. The inhibitory effect of SA treatment on *ARR7* expression is mostly conserved amongst the accessions tested. Although further biological replicates of this experiment are necessary, this provides preliminary evidence that natural variation in Arabidopsis influences CK- and SA-regulated transcriptional responses.

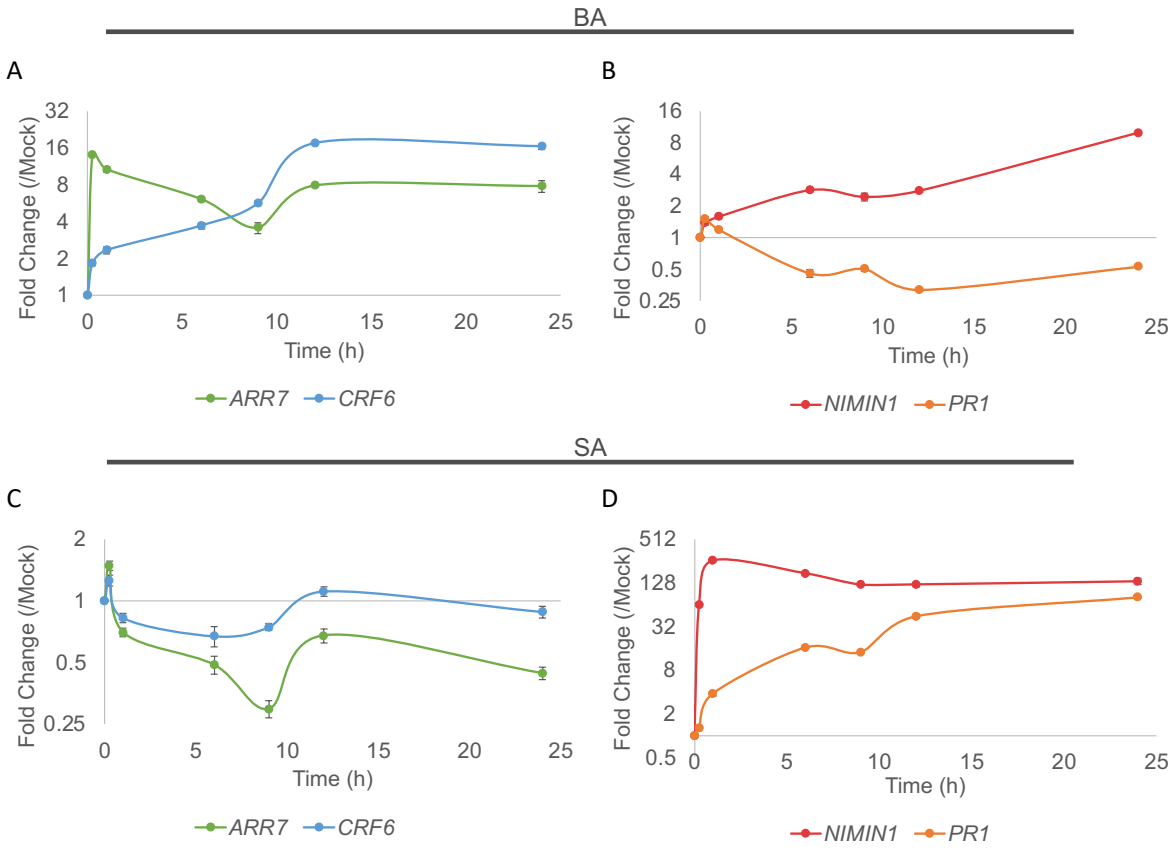

Figure 15: Modeling the CK-SA crosstalk using marker gene expression as a proxy for signaling levels. (**A**) and (**B**) gene expression after 100 µM BA treatment over a 24 h period. (**C**) and (**D**) gene expression after 100 µM SA treatment over a 24 h period. (**A**), (**B**), (**C**), and (**D**) Wildtype seedlings were grown on 1X MS plates in growth chambers in long day conditions (16 h light/8 h dark, 22°C). Light intensity was 120-150 µE. Relative humidity was held at 55% day/65% night. Fourteen days after germination, seedlings were transferred to liquid MS and allowed to acclimate for 1 h on a shaker at 75 rpm. SA, or solvent DMSO, were added to liquid culture to a final concentration of 100 µM SA in 0.01% DMSO, or 0.01% DMSO mock control. RNA was extracted from tissue collected at 0.25, 1, 6, 9, 12, and 24 h after hormone treatment, subjected to quality control, and cDNA made, followed by analysis of gene expression by qRT-PCR. Levels of *ARABIDOPSIS RESPONSE REGULATOR 7* (*ARR7*), *CYTOKININ RESPONSE FACTOR 6* (*CRF6*), *NIM1-INTERACTING 1* (*NIMIN1*), and *PATHOGENESIS-RELATED 1* (*PR1*) transcripts were determined by qRT-PCR relative to DMSO mock treatment. Error bars represent SE from three biological replicates and correspond to upper and lower limits of 95% confidence intervals. For better visualization, the axes are $\log_2$-transformed. Data shown are three independent biological replicates pooled.

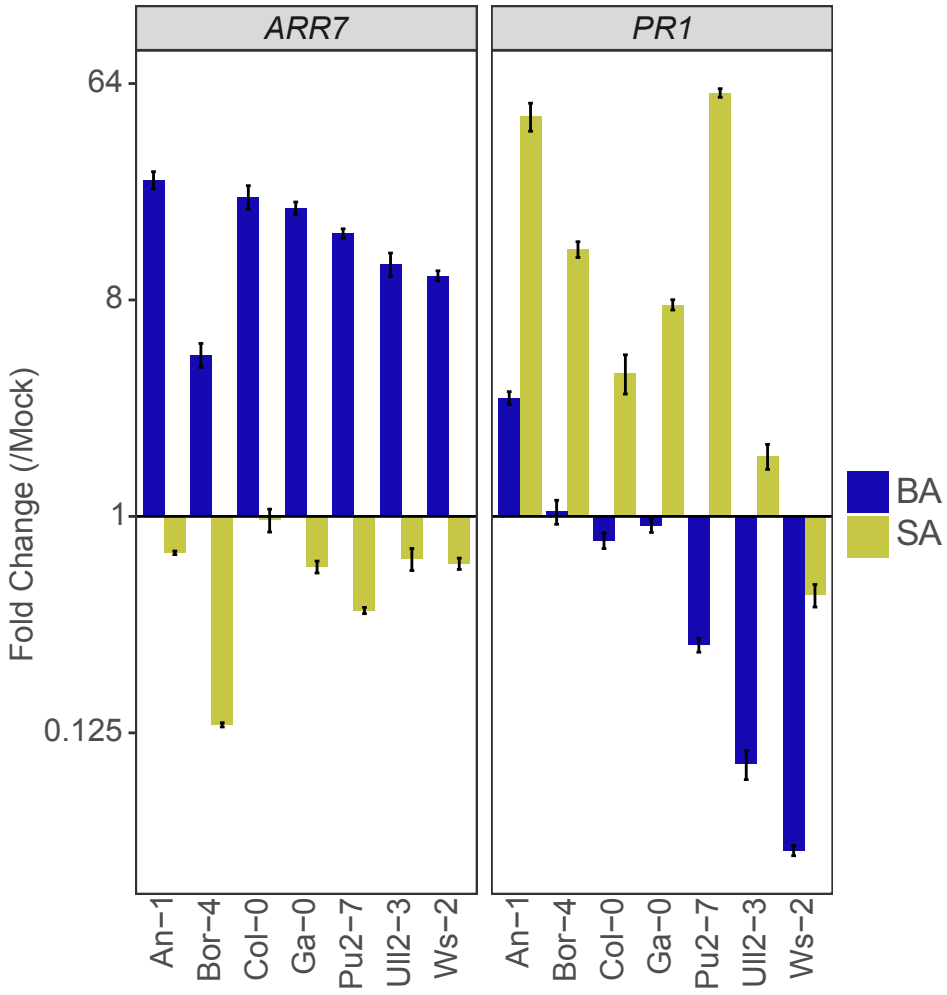

Figure 16: Arabidopsis accessions with natural genetic variation have varied responses to hormone treatment. *ARABIDOPSIS RESPONSE REGULATOR 7* (*ARR7*) and *PATHOGENESIS-RELATED 1* (*PR1*) gene expression after 100 μM BA (blue) and 1 mM SA (green) treatments. Seedlings were grown on 1X MS plates for 14 days. Plates were flooded with the corresponding hormone solution, and tissue was collected 3 h after treatment. Levels of the indicated transcripts were determined by qRT-PCR relative to mock-treated plants and normalized to *UBIQUITIN 10* (*UBQ10*). Error bars represent SE from three technical replicates and correspond to upper and lower limits of 95% confidence intervals. For better visualization, the axis is $\log_2$-transformed. Data from single biological replicate shown.

Table 4: A subset of *Arabidopsis thaliana* accessions for crosstalk experimentation. Seed stocks acquired from Arabidopsis Biological Resource Center (ABRC; https://abrc.osu.edu/) (CS22660), listed here with stock name, accession name, and location of occurrence.

Table 4 — Subset of *Arabidopsis thaliana* accessions for crosstalk experimentation

ABRC Germplasm Stock	Accession	Location	Latitude	Longitude
CS22626	An-1	Belgium	N51-N52	E4-E5
CS22591	Bor-4	Czech Republic	N49	E16
CS22625	Col-0	Missouri, USA	N38-N39	W92-W93
CS22634	Ga-0	Germany	N50-N51	E8
CS22592	Pu2-7	Czech Republic	N49	E16
CS22587	Ull2-3	Sweden	N56	E13
CS22659	Ws-2	Russia	N52-N53	E30

Discussion

We collected preliminary data in effort to examine the CK-SA relationship, using marker gene expression as a proxy for signaling levels of each hormonal pathway. The Col-0 accession was used to capture response to hormone application over time. CK treatment had a negative impact on SA signaling (Figure 15B). Although this is contradictory to previous findings where CK potentiates SA signaling, (Choi et al., 2010; Argueso et al., 2012) such work was performed in the presence of pathogens, while our experiments were performed under sterile conditions and high nutrient levels present in MS media. Another potential explanation for this incongruity is plant age. A plant's progression through the stages of development is known to be accompanied by major transcriptional reprogramming, allowing for normative growth in a given environment. In many cases, hormones direct this adaptability in a dynamic manner throughout a plant's life. For instance, younger plants are more susceptible to pathogen attack compared to mature plants; this is called age acquired resistance (ARR) and is accompanied by enhanced SA accumulation and defense responses in older plants (reviewed in Carella, Wilson, & Cameron, 2015). It is possible that younger plants, like the ones used in our assays, prioritize growth over defense, thus explaining the negative effect of CK on SA. It also bares mentioning that these experiments represent continuous exposure to hormone treatment. This is likely not reflective of endogenous hormone levels unless there is ectopic induction of these hormones. Conversely, our results show that SA treatment downregulates CK-responsive genes (Figure 15C). These data align with our findings in Figure 1. Thus, even with the differences in treatment, plant age, and experimental design between this work and previous findings (Choi et al., 2010; Argueso et al., 2012), the inhibitory effect of SA on CK signaling was observed, suggesting that this hormonal interaction is robust.

Just as different accessions have varying basal concentrations of hormones, including CK (Samsonová et al., 2020), stark growth differences (González et al., 2020), and varied susceptibility to pathogen attacks (Kerwin et al., 2015), we hypothesized that there is also

natural genetic variation in the CK-SA crosstalk amongst different accessions, as a way to overcome environment-specific selective pressures in growth and defense. Our preliminary experiment evaluating marker gene expression after hormone treatment showed differences in response to these hormones between a selection of seven Arabidopsis accessions (Figure 16), validating this hypothesis. In the future, we intend to expand our experimentation to more accessions and use marker gene expression as proxy for CK-SA crosstalk, allowing this data to be our readout for a GWA study. Mutagenesis and genetic perturbation analyses would then validate identified loci. We hope to obtain novel candidate genes implicated in the relationship between these two hormones. Ultimately, the generation of this data will allow for greater mechanistic understanding of CK-SA crosstalk, and its manipulation for the generation of enhanced plants with increased yield and resistance to pathogens.

References

Altmann, M., Altmann, S., Rodriguez, P. A., Weller, B., Elorduy Vergara, L., Palme, J., Marín-de la Rosa, N., Sauer, M., Wenig, M., Villaécija-Aguilar, J. A., Sales, J., Lin, C.-W., Pandiarajan, R., Young, V., Strobel, A., Gross, L., Carbonnel, S., Kugler, K. G., Garcia-Molina, A., … Falter-Braun, P. (2020). Extensive signal integration by the phytohormone protein network. *Nature*, *583*(7815), 271–276. https://doi.org/10.1038/s41586-020-2460-0

Argueso, C. T., Ferreira, F. J., Epple, P., To, J. P. C., Hutchison, C. E., Schaller, G. E., Dangl, J. L., & Kieber, J. J. (2012). Two-Component Elements Mediate Interactions between Cytokinin and Salicylic Acid in Plant Immunity. *PLoS Genetics*, *8*(1), e1002448. https://doi.org/10.1371/journal.pgen.1002448

Berardini, T. Z., Reiser, L., Li, D., Mezheritsky, Y., Muller, R., Strait, E., & Huala, E. (2015). The arabidopsis information resource: Making and mining the "gold standard" annotated reference plant genome: Tair: Making and Mining the "Gold Standard" Plant Genome. *Genesis*, *53*(8), 474–485. https://doi.org/10.1002/dvg.22877

Blanco, F., Salinas, P., Cecchini, N. M., Jordana, X., Van Hummelen, P., Alvarez, M. E., & Holuigue, L. (2009). Early genomic responses to salicylic acid in Arabidopsis. *Plant Molecular Biology*, *70*(1–2), 79–102. https://doi.org/10.1007/s11103-009-9458-1

Cammarata, J., Morales Farfan, C., Scanlon, M. J., & Roeder, A. H. K. (2022). Cytokinin–CLAVATA cross-talk is an ancient mechanism regulating shoot meristem homeostasis in land plants. *Proceedings of the National Academy of Sciences*, *119*(14), e2116860119. https://doi.org/10.1073/pnas.2116860119

Carella, P., Wilson, D. C., & Cameron, R. K. (2015). Some things get better with age: Differences in salicylic acid accumulation and defense signaling in young and mature Arabidopsis. *Frontiers in Plant Science*, *5*. https://doi.org/10.3389/fpls.2014.00775

Clark, N. M., Nolan, T. M., Wang, P., Song, G., Montes, C., Valentine, C. T., Guo, H., Sozzani, R., Yin, Y., & Walley, J. W. (2021). Integrated omics networks reveal the temporal

signaling events of brassinosteroid response in Arabidopsis. *Nature Communications*, *12*(1), 5858. https://doi.org/10.1038/s41467-021-26165-3

D'Agostino, I. B., Deruère, J., & Kieber, J. J. (2000). Characterization of the Response of the Arabidopsis Response Regulator Gene Family to Cytokinin. *Plant Physiology*, *124*(4), 1706–1717. https://doi.org/10.1104/pp.124.4.1706

Hirschhorn, J. N., & Daly, M. J. (2005). Genome-wide association studies for common diseases and complex traits. *Nature Reviews Genetics*, *6*(2), 95–108. https://doi.org/10.1038/nrg1521

Liu, J., Rowe, J., & Lindsey, K. (2014). Hormonal crosstalk for root development: A combined experimental and modeling perspective. *Frontiers in Plant Science*, *5*. https://doi.org/10.3389/fpls.2014.00116

Matthews, M. L., & Marshall-Colón, A. (2021). Multiscale plant modeling: From genome to phenome and beyond. *Emerging Topics in Life Sciences*, *5*(2), 231–237. https://doi.org/10.1042/ETLS20200276

Middleton, A. M., Úbeda-Tomás, S., Griffiths, J., Holman, T., Hedden, P., Thomas, S. G., Phillips, A. L., Holdsworth, M. J., Bennett, M. J., King, J. R., & Owen, M. R. (2012). Mathematical modeling elucidates the role of transcriptional feedback in gibberellin signaling. *Proceedings of the National Academy of Sciences*, *109*(19), 7571–7576. https://doi.org/10.1073/pnas.1113666109

Proietti, S., Caarls, L., Coolen, S., Van Pelt, J. A., Van Wees, S. C. M., & Pieterse, C. M. J. (2018). Genome-wide association study reveals novel players in defense hormone crosstalk in *Arabidopsis*: Genome-wide association mapping of hormone cross-talk genes. *Plant, Cell & Environment*, *41*(10), 2342–2356. https://doi.org/10.1111/pce.13357

Prusinkiewicz, P., & Runions, A. (2012). Computational models of plant development and form. *New Phytologist*, *193*(3), 549–569. https://doi.org/10.1111/j.1469-8137.2011.04009.x

Rashotte, A. M., Mason, M. G., Hutchison, C. E., Ferreira, F. J., Schaller, G. E., & Kieber, J. J. (2006). A subset of *Arabidopsis* AP2 transcription factors mediates cytokinin responses in concert with a two-component pathway. *Proceedings of the National Academy of Sciences*, *103*(29), 11081–11085. https://doi.org/10.1073/pnas.0602038103

Samsonová, Z., Kiran, N. S., Novák, O., Spyroglou, I., Skalák, J., Hejátko, J., & Gloser, V. (2020). Steady-State Levels of Cytokinins and Their Derivatives May Serve as a Unique Classifier of Arabidopsis Ecotypes. *Plants*, *9*(1), 116. https://doi.org/10.3390/plants9010116

Sheflin, A. M., Kirkwood, J. S., Wolfe, L. M., Jahn, C. E., Broeckling, C. D., Schachtman, D. P., & Prenni, J. E. (2019). High-throughput quantitative analysis of phytohormones in sorghum leaf and root tissue by ultra-performance liquid chromatography-mass spectrometry. *Analytical and Bioanalytical Chemistry*, *411*(19), 4839–4848. https://doi.org/10.1007/s00216-019-01658-9

Sheth, B. P., & Thaker, V. S. (2014). Plant systems biology: Insights, advances and challenges. *Planta*, *240*(1), 33–54. https://doi.org/10.1007/s00425-014-2059-5

Soualiou, S., Wang, Z., Sun, W., de Reffye, P., Collins, B., Louarn, G., & Song, Y. (2021). Functional–Structural Plant Models Mission in Advancing Crop Science: Opportunities and Prospects. *Frontiers in Plant Science*, *12*, 747142. https://doi.org/10.3389/fpls.2021.747142

Ward, E. R., Uknes, S. J., Williams, S. C., Dincher, S. S., Wiederhold, D. L., Alexander, D. C., Ahl-Goy, P., Metraux, J. P., & Ryals, J. A. (1991). Coordinate Gene Activity in Response to Agents That Induce Systemic Acquired Resistance. *The Plant Cell*, 1085–1094. https://doi.org/10.1105/tpc.3.10.1085

Yuan, J. S., Galbraith, D. W., Dai, S. Y., Griffin, P., & Stewart, C. N. (2008). Plant systems biology comes of age. *Trends in Plant Science*, *13*(4), 165–171. https://doi.org/10.1016/j.tplants.2008.02.003